KONSTANTIN DOUBROVINSKI

Developing a model for dynamic relocation of Soj in *Bacillus subtilis*

Master's degree project

Molecular Biotechnology Programme

Uppsala University School of Engineering

UPTEC X 04 45	Date of issue 2004-11
Author **Konstantin Doubrovinski**	

Title (English)
Developing a model for dynamic relocation of Soj in *Bacillus subtilis*

Title (Swedish)

Abstract   The mechanisms used to self-organize complex subcellular structures are of vital importance in biology, but are nevertheless poorly understood. In this study we examine a key example of bacterial self-organization, namely internucleoid jumping of the Soj protein in *Bacillus subtilis*. We develop a mathematical model, with assumptions based closely on experiment, to explain the Soj jumping via a dynamical instability.

Keywords   Soj, Spo0J, dynamic oscillations, self-organization, reaction-diffusion

Supervisors   **Dr. Martin Howard**   Department of Mathematics, Imperial College London
Scientific reviewer   **Prof. Otto Berg**   Department of Evolution, Genomics and Systematics at Uppsala University, Sweden   **Dr. Torgny Fornstedt**   Department of Surface Biotechnology at Uppsala University, Sweden

Project name	Sponsors
Language **English**	Security **12 months**
ISSN 1401-2138	Classification
Supplementary bibliographical information	Pages **43**

Developing a model for dynamic relocation of Soj in *Bacillus subtilis*

Sammanfattning

Mekanismer som möjliggör noggrann reglering av de intracellulära processerna har länge fascinerat biologer. Tack vare nya experimentella tekniker har man på senare tid kunnat fullt uppskatta den höga graden av organisationen på intracellulära strukturer. Hur denna uppnås är en fråga av fundamentalt intresse inom biologin.

I detta arbete har vi försökt att närma oss problemet genom att studera dynamiken hos ett protein Soj som uppvisade regelbundna "oscilleringar" inuti den avlånga bakteriecellen. Genom att använda oss utav matematiska modeller och numerisk modellering har vi lyckats visa att ytterst enkla antaganden baserade uteslutande på experimentellt framtagen data gör det möjligt att förklara proteinets dynamiska uppförande. Vårt arbete ger ett biologiskt relevant exempel på självorganisation i komplexa system där hela systemet visar sig vara mycket mer än summan av sina beståndsdelar.

Examensarbete 20 p i Molekylär bioteknikprogrammet

Uppsala universitet november 2004

Developing a Model for Dynamic Relocation of Soj in *Bacillus subtilis*

Introduction

The term "pattern formation" designates a physical process whereby a coherent structure arises starting from random initial conditions. Usually, the coherence lies in spatial or temporal periodicity. Numerous examples of systems exhibiting pattern formation have been described in various areas of physics. Coupled chemical reactions with regularly oscillating concentrations of several compounds; heterogeneous catalysis yielding intricate periodic patterns and complicated structures in fluid convection, are a few examples of this remarkable phenomenon.

Usually, pattern formation involves interactions between several different components of a physical system. For example in the case of chemical kinetics and heterogeneous catalysis, different species diffuse and react with each other, yielding spatial or temporal periodicity. The description of individual interactions usually does not pose any particular difficulty. However, the emergence of the pattern relies on putting together all of the intricate interactions, involving collective, coherent self organization. Therefore, in order to understand the behaviour of such complex systems one is frequently forced to adopt numerical modelling.

In recent decades a great deal of work has been done on pattern forming chemical systems. A wealth of experimental information and theoretical examinations has been put forward. However, only in recent years has one started to apply these methods to modelling the pattern forming behaviour of biological systems. The major reason for this is the lack of quantitative data.

Here we will concentrate on oscillatory pattern-forming behaviour of proteins in prokaryotes. Let us first recapitulate some of the earlier work conducted in this area.

In the work by Howard *et al* (Howard *et al*., 2001), a pattern forming oscillatory system comprised of three proteins, namely MinC, MinD and MinE, is described. Genetic experiments demonstrated that MinC remained cytoplasmic in the absence of MinD. MinD serves to recruit MinC to the membrane. This system turned out to produce remarkable oscillations. MinC together with MinD first assembles at one end of the cell. MinE, initially localized at the mid-cell, moves towards the cell pole and ejects MinC and MinD into the cytoplasm. As MinD and MinC reassemble at the opposite pole, the process is repeated. Based on this experimental evidence, the authors put forward a system of reaction-diffusion equations, faithfully reproducing the observed dynamics. The remarkable feature of this model was the conservation of total protein amounts. Most of the models describing chemical pattern formation rely on the presence of constant inflow and outflow of some components. Furthermore, Howard and co-workers explored the mechanism of pattern formation, showing that it appeared to be so-called Turing-instability. This shows that the oscillatory pattern is

likely to emerge, regardless of initial conditions. Importantly, the authors show that the model predicts the presence of a time average minimum of MinC and MinD concentration at midcell. It was known that MinC inhibited the formation of the FtsZ-ring, a structure marking the division site. Consequently, the MinCDE system serves to locate the middle of the bacterial cell and ensures accurate cell division solely by means of interactions between reacting and diffusing particles, in the absence of any distinct marker. In later work, the authors conducted Monte-Carlo simulations, examining the influence of noise on the dynamics. It turned out that oscillations could persist even in parameter ranges where no dynamics was observed in the deterministic model.

In another paper by Howard (Howard, 2004) the author attempts to explain the mechanism of polar localization of MinD in *B. subtilis*. In this case the appropriate distribution of protein particles could in principal be achieved in the same manner as in *E. coli*, as described above. However, no oscillatory dynamics of Min proteins was observed in this bacterium. The author puts forward a different reaction-diffusion model, based on the experimental evidence from GFP fusion and deletion mutants, capturing the interactions of proteins called MinD and DivIVA. The results of numerical modelling give a plausible explanation of polar localization of these proteins. During vegetative growth the initial distribution of the protein of the mother cell can, in principle, control the targeting of MinD and DivIVA in the daughter cells. However, this mechanism would not account for appropriate localization of these proteins in outgrowing spores. Furthermore, the patterns seen in the simulations are very similar to the distribution of, for example, the McpA chemotaxis receptor protein in *C. crescentus*. So, the model suggested in the article could have greater applicability.

In an article by Hunding *et al* (Hunding *et al.*, 2003) the authors outline a number of general mechanisms explaining the emergence of protein localization patterns in bacteria. Several protein interaction networks are described and the possibility of spatiotemporal self-organization is assessed in each case. This is done by means of numerical simulation as well as by means of linear stability analysis, similar to the one we conduct below. Moreover some features like the conservation of total protein amounts, the presence of quadratic cooperativity (that is to say that the rate of binding of certain reactants is proportional to the square of the concentration of the bound form), and the overall structure of the equations, are very similar to those of the model we describe.

Recapitulation of the earlier experimental work

In recent years much effort has been undertaken in order to clarify the mechanism of accurate nucleoid segregation of bacterial cells. Experimental research in this area revealed that the origins of the two bacterial chromosome move apart abruptly towards the opposite cell poles soon after replication initiates. The chromosomal origin has a precisely defined orientation during chromosomal segregation, indicating the presence of a mitotic-like segregation apparatus. (Chi-Hong Lin *et al.*, 1998). The high fidelity of segregation and relatively small frequency of anucleate cells also implies the requirement of active segregation machinery. (Glaser *et al.*, 1997) Nevertheless, all of the components of such a mechanism have not yet been unambiguously identified. (Autret *et al.*, 2001).

However, the ParAB family of proteins have long been known to play an important role in this context. Their homologues have been identified in a great number of bacteria, including *Pseudomonas putida*, *Caulobacter crescentus*, *Streptomyces coelicolor*, *Streptococcus pneumoniae*, *Mycobacterium leprae*, *Helicobacter pylori* and *Streptococcus pyogenes* suggesting that they are widely conserved across bacterial species. As with many other cellular components, these polypeptides are involved in a whole range of cellular processes. Initially, these macromolecules were shown to be required for stabilizing an unstable plasmid.

Complexes of ParB proteins, associated with bacterial plasmids have been visualized by means of fluorescence microscopy. These structures have been described as bright, distinct patches, moving and separating upon cell cycle progression, again suggesting the presence of a mitotic-like apparatus, facilitating chromosome segregation. However, the data on the details of this process is rather scarce.

The function of ParA proteins has also remained elusive. These macromolecules have been known to contain Walker A and Walker B boxes, characteristic for ATPases (Walker *et al*., 1982). ATP hydrolysis has also been demonstrated in vitro by means of biochemical methods. Moreover, ParA family proteins are involved in DNA binding. (Marston *et al*., 1999)

In *Bacillus subtilis* the homologues of ParA and ParB are called Soj and Spo0J respectively. Spo0J was shown to bind to *parS sites*, localized in the origin proximal 20 % of the chromosome. When a *parS site* is incorporated into a separate plasmid, Spo0J interactions are required for plasmid stabilization. Furthermore, upon deleting Spo0J the frequency of anucleate cells increases some hundredfold, clearly implying that Spo0J is important for faithful chromosome segregation. The role of Soj in chromosome partitioning remains unclear. However, this macromolecule was shown to be required in combination with Spo0J for effective plasmid stabilization.
Moreover both Soj and Spo0J are involved in sporulation control. A null mutation in spo0J suppresses sporulation. Deleting Soj relieves this defect. This experimental data suggests that Soj acts as a suppressor of early sporulation genes, while Spo0J antagonizes its effect.

By means of crystallographic studies, one can put forward a plausible mechanism describing Spo0J-DNA interactions. (Leonard *et al*., 2004) This protein turned out to have a rather compact conformation, containing approximately 65 % alpha-helices, exhibiting clear similarity to the HTH motif to the DNA-binding domain of the lambda repressor. The authors claim that the crystal structure of Spo0J consists of dimers, held together primarily by means of a hydrophobic interaction between the N-terminal part of one monomer and C-terminal part of the other. Furthermore, the distance between the DNA binding domains within a dimer is approximately the same as the distance between two successive major grooves of DNA. Moreover, it turned out that while the C-terminal showed signs of dimerization in the solution, the N-terminal domains did not dimerize. Rather, the presence of the N-terminal domain inhibited the formation of C-terminal domain dimers. Based on this experimental data Leonard and co-workers put together a number of similar mechanisms explaining the details of Spo0J-DNA interactions. They suggest that different protein particles

undergo DNA-dependent dimerization on the surface of the DNA template, interlocking with each other by means of interactions between the C-terminal domains.

Spo0A is another protein involved in regulation of sporulation. Its presence enhances sporulation and Soj has the ability to antagonize the effects of this protein. Therefore, the Soj mode of action appears to be indirect to a certain extent. (Quisel *et al*., 1999).

There are several other cellular components, apart from the ParAB protein family, whose involvement in cell division control is of relevance for the following discussion. Depleting the bacterial protein FtsZ abolishes cell division. Cells lacking this molecule will grow without dividing. In this way long filamentous cells are produced. In wild type cells, FtsZ forms a characteristic ring structure at mid-cell, marking the future division site. This ring never localizes in close proximity to the nucleoids due to a poorly understood mechanism, called nucleoid occlusion. Moreover, FtsZ never assembles near the cell pole. This is assured by its interactions with other vital proteins, MinC and MinD. MinC was identified as an actual inhibitor of FtsZ assembly. MinC localizes at the cell pole by means of interactions with MinD, which is a membrane associated ATPase. MinD is anchored at the cell pole by another protein, called DivIVA. (Autret *et al*., 2003).

Experimental background

It has previously been suspected that Soj is capable of repressing the expression of many early sporulation genes, for example *spoIIA*, *spoIIG* and *spoIIE*. In the paper by Quisel *et al* (Quisel *et al*., 1999), the authors give a detailed investigation of the mechanism of this repression. In a so-called cross-linking experiment one allows the protein to covalently bind to DNA in presence of formaldehyde. Then, the cells are lysed, and a specific protein of interest is recovered by means of immunoprecipitation. The presence of certain DNA fragments, associated with the recovered protein is assessed by means of PCR. In this way, the authors have been able to demonstrate an association of Soj with the above mentioned promoters *in vivo*. Moreover, by diluting the sample before amplifying the DNA fragments with PCR, one can quantify the amounts of DNA associated to a given protein. Interestingly, deleting *spo0J* resulted in a fourfold increase in Soj binding to the promoters of the sporulation genes. In summary, Soj is capable of spontaneous association with DNA and this binding is repressed in the presence of Spo0J.

By means of GFP (green fluorescent protein) fusion and subsequent fluorescence microscopy one can determine the subcellular localization of a protein. The gene expressing the protein of interest is first fused in frame with *gfp*. The resulting protein is then capable of emitting light when illuminated in the ultraviolet. In this way Quisel and co-workers determined that Soj predominantly localizes at the cell pole, forming small characteristic band-shaped foci. Furthermore, disrupting *spo0J* made these structures disappear. Instead, all the Soj formed a diffuse patch at midcell. The position of this patch was practically identical with that of the nucleoid. Therefore, the authors suggested that Spo0J expels Soj from the nucleoid, forcing it to localize at the cell pole.

Time-lapse experiments demonstrated that Soj is capable of remarkable dynamical relocation from one end of the cell to the other and back. The dynamics is captured in

time-lapse images, pictured in the article. Basically, the patch at one end of the cell disappears and re-emerges at the other after several minutes.

More deliberate site-directed mutagenesis experiments have helped identify the domains of the proteins that are vital for its function. Such experimental procedures are of great value, when details of protein-protein interactions have to be untangled. Among other mutation analysis conducted by Quisel and co-workers two are of primary interest. The first one is in the so-called Walker box, rendering Soj unable to bind to nucleotides (ATP or ADP). The other mutation is expected not to affect the nucleotide binding ability of Soj, but decrease the rate of nucleotide exchange. When it comes to sporulation, both mutants showed similar phenotype: they bypassed the need of Spo0J for sporulation.

However, while the first strain, bearing mutation in the Walker box, displayed an altered pattern of Soj localization (Soj no longer associated with the cell pole), the Soj still assembled at the cell pole in the mutant defective in nucleotide exchange. This suggests that Soj requires nucleotide binding in order to localize at the cell end, but nucleotide exchange is needed for Soj efficient suppression of sporulation. Finally, both mutations abolished dynamic relocations of Soj.

The work by Marston *et al* (Marston *et al*., 1999) gives further information on the nature of Soj-Spo0J interactions. The details of the reorganization and localization of Spo0J in absence and presence of Soj are of great interest for this discussion.
It has previously been known from the studies of plasmid encoded ParAB-family proteins that ParA is involved in restructuring ParB assemblies. In order to clarify this issue in the case of Soj-Spo0J interaction, Marston and co-workers constructed a Spo0J-GFP fusion. Subsequent fluorescence microscopy revealed that Spo0J-GFP colocalized with every nucleoid, forming a bright, characteristic patch. As Spo0J predominantly binds to the origin proximal region and the examined cells usually contain two origins, Spo0J was found to localize in a special bipolar pattern with two patches per cell.

Upon deleting *soj*, the Spo0J patches disappeared. In this case Spo0J showed significantly more dispersed localization. This suggests that Soj promotes the condensation of Spo0J foci. The paper is supplemented with excellent fluoro-micrographs, illustrating this remarkable behaviour.

Also, Soj localization was assessed by Marston and co-workers. They showed that Soj of the wild type cells is predominantly associated in a large bright nucleoid associated patch. These patches usually marked one of several bacterial chromosomes and they were far less condensed than the Spo0J foci. Some background cytoplasm signal was present, suggesting that some Soj remained in the cytoplasm.
Further investigations, using nalidixic acid which perturbs DNA replication without influencing cell growth, gave unambiguous evidence of Soj-DNA association.

Time-lapse experiments were also conducted. Just as described by Quisel *et al*, dynamical flip-flops from one nucleoid to the adjacent one on a timescale of minutes was observed. The Soj relocations happened extremely rapidly, that is to say the time it took to relocate from one nucleoid to the proximal one was much shorter then the time Soj remained in the nucleoid-associated form. This suggests that some stage of

this dynamical process is highly cooperative, meaning that its further progression is enhanced by the presence of the accumulating component.

Again, as was described in the previous (Quisel *et al*., 1999) paper, Marston *et al* point out that the Soj oscillations were abolished in the absence of Spo0J.

Another important experiment was conducted by this research group. FtsZ is the protein which assembles in a ring at the mid-cell prior to cell division. This peculiar ring structure marks the site of cell division. Upon deleting FtsZ, cell division no longer occurs, but DNA replication proceeds unperturbed. This way abnormally long cells with as many as eight to sixteen nucleoids can be produced. The pattern of Soj localization in this mutant is of course of great interest. It turned out that all of the Soj now assembled on one single nucleoid in a very bright focus (presumably because of the increased total amount of protein in the long filaments). Interestingly this patch preferentially assembled on the nucleoid positioned closest to the cell pole, rather than at any random chromosome. This suggests that Soj must interact with some cellular component which predominantly localizes near the cell end. Time-lapse experiment showed no signs of the characteristic Soj oscillations.

Finally, most of the Spo0J was uncondensed in this mutant, again suggesting that Soj is directly involved in Soj condensation.

In the paper by Autret (Autret *et al*., 2003) another cellular component influencing Soj oscillations was identified. Two proteins, MinC and MinD localize at the cell pole. MinD is an ATPase and is held in place by interactions with DivIVA. As mentioned above, MinC interacts with FtsZ, ensuring that the FtsZ ring assembles only at the mid-cell and, consequently, both daughter cells become equally long. Disrupting either MinC or MinD causes cells to become somewhat longer than the wild type. In this case the cells were far shorter than the long FtsZ filaments, containing around four nucleoids. The effects of deleting MinC and those of deleting MinD were virtually indistinguishable when it comes to cell length alteration. Yet, disrupting MinD abolished Soj jumps, whereas *minC* deletion also perturbed the Soj relocations, but not to the same extent. This experimental data suggests that MinD is required for generating the oscillations and that this effect is not entirely due to the changes of the cell length.

In order to gain a better understanding of Soj interactions with the cell pole, long filamentous cells lacking MinD were constructed and the Soj localization pattern of these cells was compared to that of the long filaments lacking FtsZ but containing MinD. It turned out that in both cases all the Soj assembled in a single bright patch on one chromosome. However, while this patch preferably localized on the cell proximal nucleoid in the cells containing MinD, the Soj assembled on a random nucleoid in the mutants lacking MinD.

Finally, this paper describes an investigation of a previously isolated mutant in which ATP hydrolysis was impaired (the same mutant as described (Quisel *et al*., 1999) by Quisel *et al*). In long *ftsZ* filaments containing MinD, Soj formed distinctive narrow bands near the cell ends just as it did in the normal length cells.

In summary, these last observations suggest that after disassociating from the nucleoid Soj has to go to the cell pole and undergo MinD promoted nucleotide exchange in order to rebind to the DNA. This also explains the fact that the Soj patch is frequently

found near the cell end in long filaments, while it localizes at a random chromosome in cells lacking MinD.

The requirement of nucleotide exchange at the cell pole for efficient Soj relocations was pointed out by Quisel *et al* in the article mentioned above. In the same paper the authors suggest that Soj binds DNA in the ADP form and acquires a phosphate upon unbinding. ATP hydrolysis at the cell end allows Soj to rebind. However unpublished results by Löwe (personal communications) unambiguously determine that Soj binds DNA in the ATP form. So, it is more likely that Soj undergoes hydrolysis upon dissociation from DNA while phosphorylation occurs at the cell end.

Finally, the paper by Autret (Autret *et al*., 2001) provides yet another vital experimental observation of great relevance to our study. In this work, Autret and co-workers describe a selection of Spo0J mutants, constructed by means of random as well as site directed mutagenesis.

Most of the mutations significantly impaired nucleoid morphology. Two major types of defects were identified: increase in the frequency of anucleate cells and elongated cells with abnormally condensed nucleoids. One of the mutants, however, did not display appreciable chromosome segregation defects.

The ability of mutants to sporulate was assessed by monitoring the production of alkaline phosphatase, an enzyme which is predominantly synthesized during the so called stage II of sporulation. All mutants turned out to be defective in sporulation except for the one which did not display a significant chromosome segregation defect.

Moreover, the effects of mutations on the morphology of Spo0J foci were determined. In the mutant, displaying normal segregation and sporulation, the foci looked rather similar to those of the wild type. However, in all the other cases no foci were observed and Spo0J was dispersed throughout all of the cytoplasm. In yet another strain the foci did form, but they were rather diffuse and less pronounced then those of the wild type.

Furthermore, the ability of Spo0J to promote the condensation of Soj foci was assessed by means of GFP-fusion and fluorescence microscopy. It turned that the pattern of Soj localizations in the mutants was virtually indistinguishable from that of *spo0J* strain. Soj remained stably associated with the nucleoid.

One of the mutants was a good candidate for examining the dynamical behaviour of Soj relocations, as neither segregation, nor sporulation, nor was the formation of Soj foci significantly impaired. Time-lapse experiments indicated that Soj relocations are somewhat more frequent in these cells. As was mentioned previously, depleting FtsZ and consequently preventing subsequent cell division abolished the oscillations. This was not the case for this remarkable strain.

Methods

The main purpose of this investigation is to put forward a mathematical model which is capable of reproducing most of the experimental facts summarized above. The experimental data can be rationalized in order to illuminate the mechanism of the

oscillation. As mentioned previously, Soj spontaneously associates with the DNA, subsequently repressing the transcription of the early sporulation genes. Cross-linking experiments demonstrated that this binding is inhibited by Spo0J. Furthermore, Spo0J is unable to assemble into the characteristic bright foci in the absence of Soj. We suggest the following mechanism of oscillation. Assume that initially Soj is found in the cytoplasm. Spontaneous binding of Soj to the nucleoid promotes Spo0J condensation. Then, condensed Spo0J expels Soj from DNA and subsequently decondenses. Now the system is in its initial configuration and the cycle repeats. Furthermore, as there are two nucleoids in each bacterial cell, the Soj is able to reassemble on the adjacent chromosome as it gets expelled from the first one by Spo0J. Therefore the oscillations are from nucleoid to nucleoid rather than from nucleoid to cytoplasm. The mechanism of oscillations is comprehensively summarized in figure (1).

Of course, the choice of model is the most difficult step one is confronted with when it comes to modelling the dynamics described above. A simple ordinary differential kinetic rate equations can be used as a first step. Unfortunately, such a model will be unable to capture spatial variation in the concentration of proteins. However, we know that the period of the observed Soj relocation is several minutes, while a customary value of a diffusion constant for an average size protein in the bacterial cytoplasm is approximately 2 μm^2/s.

Therefore diffusion is not the rate determining step and we can initially neglect spatial variation in protein concentration levels. Ordinary Differential Equations (ODE) are therefore still appropriate.

The most immediate choice of a model, encompassing the experimental facts, would probably be:

$$\frac{\partial So}{\partial t} = -k_1 So - k_1 So + k_2 (so_1)(sp_1) + k_2 (so_2)(sp_2)$$

$$\frac{\partial so_1}{\partial t} = k_1 So - k_2 (so_1)(sp_1)$$

$$\frac{\partial so_2}{\partial t} = k_1 So - k_2 (so_2)(sp_2)$$

$$\frac{\partial Sp_1}{\partial t} = k_3 sp_1 - k_4 (Sp_1)(so_1) \qquad (1)$$

$$\frac{\partial sp_1}{\partial t} = -k_3 sp_1 + k_4 (Sp_1)(so_1)$$

$$\frac{\partial Sp_2}{\partial t} = k_3 sp_2 - k_4 (Sp_2)(so_2)$$

$$\frac{\partial sp_2}{\partial t} = -k_3 sp_2 + k_4 (Sp_2)(so_2)$$

Where *So* represents the concentration of cytoplasmic Soj, *so_1* is the concentration of Soj assembled on the first nucleoid, *so_2* is the concentration of Soj on the second chromosome. Finally, *Sp_1* and *sp_1* (*Sp_2* and *sp_2*) are the concentrations of Spo0J in uncondensed and condensed forms respectively assembled on the first (second) nucleoid. One particularly "pleasant" property of the above equations is that they

preserve total protein amounts. Indeed, if we add the first three equations we see that the conservation of the total Soj concentration follows. The same is of course true for the total Spo0J concentration. This statement has two interesting and functionally vital consequences. On the one hand, as protein synthesis, cell cycle progression and Soj dynamical relocations usually proceed on different time scales, no one of these processes is likely to be directly involved in driving the other one. This is reflected in the structure of the above ODE. Moreover, if the oscillations would be driven solely by means of protein synthesis, the energy expenses would be enormous. Therefore it seems extremely plausible to suggest that the basic model should conserve the total protein amounts, as is indeed the case in our description.

Many self-organizing reaction-diffusion systems such as for example Belousov-Zhabotinsky's reaction (Belousov 1958, Zhabotinsky 1964) have gained considerable attention in recent years. It is well known that in order to sustain oscillations in a chemical medium one needs to continuously feed in more reactants into the system. However, biologically it seems much more plausible that protein oscillations are driven by ATP hydrolysis rather then *de novo* protein synthesis, as the energy expenses can then be reduced by as much as a hundred- to a thousand-fold (Howard *et al.*, 2001).

One problem with constructing our mathematical description is that the nature of Spo0J condensation is poorly understood. The only information that can be extracted from the experimental articles suggests hat this process somehow involves bringing together and interlocking the different Spo0J particles bound at different locations of the chromosome. The simplest way of handling this difficulty is to assume first order kinetics. That is to say, Spo0J decondenses with a rate which is proportional to the amount of condensed protein, while it condenses with a rate proportional to the concentration of uncondensed Spo0J and that of DNA associated Soj. Again, we would like to emphasize that this is not a sufficiently detailed model of the intricate condensation process, but considering that no detailed information on this issue is available, we are forced to assume the simplest possible dynamics.

The rest of the model is rather self explanatory. The rate at which Soj binds to the nucleoid is proportional to the concentration of cytoplasmic Soj. The rate of Soj release is proportional to the amount of chromosome associated protein and to the concentration of condensed Spo0J which is expected to expel Soj from the DNA.

Now, no kinetic parameters in the above model have ever been determined. That is to say, we do not know k_1, k_2, k_3 and k_4. In principle, these constants can be acquired, for example, by means of so called stopped-flow experiments. This might constitute a subject of future research. In our case, the constants must be manually adjusted so that the dynamics of the model becomes appropriate and robust, and also so that it resembles that of the real experimental system.

Although extensive adjustments of the kinetic parameters were attempted, the model above did not yield any oscillatory dynamics. Occasionally, some parameter values yielded transitory oscillations, suggesting the presence of a stable focus in the phase space of the system. Furthermore, whenever these unstable oscillations were observed, the time of Soj relocation from one nucleoid to the other was comparable to the time that was spent in the DNA associated state.

In the description of the time-lapse experiments it was noted that all Soj disappeared from the nucleoid in a short period of time. The assembly on the proximal chromosome was also very rapid. The authors suggested that this implies the presence of cooperativity in Soj binding. That is to say, the rate at which Soj associates with the nucleoid depends on the amount of Soj already bound. Consequently, Soj binding promotes itself and rapid accumulation is achieved in this way.

In order to take these facts into account, the k_1So term in the above equation was replaced by a term of the form $k_1So(1+\sigma_1(so_1)^2)$. The degree of coperativity is now controlled by two parameters. On the one hand, the cooperativity becomes more profound upon increasing σ_1. On the other hand we choose to have quadratic cooperativity (or, equivalently, Hill coefficient 2) in order for our system to exhibit hysteresis. How this is achieved is most appropriately explained in terms of a bifurcation diagram.

Let us assume we intend to investigate the properties of an arbitrary dynamical system, given in terms of (possibly several coupled) ordinary (or partial) differential equations:

$$\frac{\partial z}{\partial t} = f(z,\mu) \qquad (2)$$

Where f is a known function, z is the dependent variable whose dependence on t is sought and μ is a parameter, independent of t. Let us further suppose that we can determine the position of the steady state in the phase plane. This is done simply by solving equation $f(z,\mu)=0$ for every fixed μ Finally, let us plot the solution of this equation against different values of μ. What we get is a bifurcation diagram. For every given value of parameter μ it depicts the position of all steady states.

Customary bifurcation diagram with hysteresis
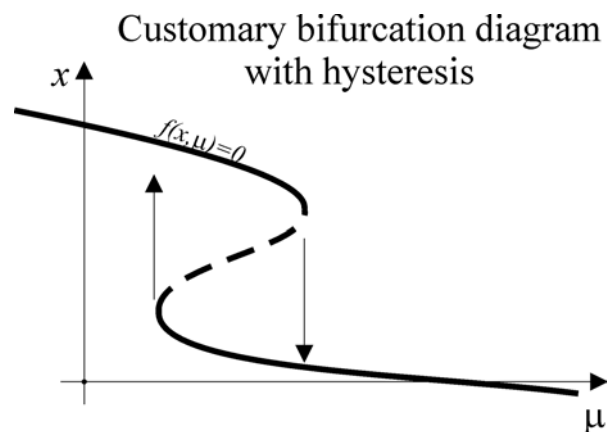
The bifurcation diagram for our system with some minor modifications is depicted in figure (2). The concentration of condensed Spo0J serves as the bifurcation parameter. It turns out that such a graph is an invaluable tool for revealing the nature of the dynamics. Suppose that initially the concentration of condensed Spo0J is high. But then the system will asymptotically approach the only available steady state with a low concentration of bound Soj. Now, the concentration of condensed Spo0J ought to decrease due to spontaneous decondensation of this protein. If this process is sufficiently slow, the concentration of Soj will follow the branch of the diagram. After

each small perturbation in Soj concentration the system approaches the corresponding steady state with the stationary concentration of DNA associated Soj given in the diagram. However, as the concentration of condensed Spo0J decreases past the "fold" of the bifurcation curve, there is no longer any stationary point of bound Soj in close proximity. Now the concentration of bound Soj will have to increase in order to return to its new stationary value. But increased concentration of DNA associated Soj must initiate Spo0J condensation, and the movement along the bifurcation branch proceeds in the opposite direction until encountering the fold of the bifurcation curve, now resulting in an abrupt drop of the concentration of bound Soj. As is seen from the diagram, the concentration of condensed Spo0J required to initiate the effective release of Soj is higher then the concentration of Spo0J at which the binding is initiated. This is called hysteresis and this mechanism is going to constitute the very heart of the model, generating a stable limit cycle in the phase plane. Clearly this would be impossible to achieve without introducing quadratic cooperativity. If the k_1-term, for example, read $k_1 So(1+\sigma_1(so_2))$ the bifurcation diagram would basically depict the position of the roots of a second order equation. No hysteresis would result as quadratic polynomial cannot have three roots. Consequently, no fold of the curve would have been found.

It is interesting to note that as kinetic rate equations with a particular type of interactions have a rather restricted form, there will be relatively few models capable of displaying stable oscillations. The term stable implies the presence of a limit cycle which is approached by any solution in some neighbourhood. For example the well known Volterra-Lotka model, describing some hypothetical oscillatory dynamics, has a limit cycle through every point of phase space. These limit cycles are unstable as any perturbation forces the system to leave one such cycle for another one, consequently changing the frequency and the amplitude of the oscillations. It has previously been shown that there only exists one three-component model with chemically reasonable stoichiometry, capable of displaying stable oscillations. (Nicolis & Prigogine 1977)

Of course, as the ODE is unable to capture spatial variations in concentration, we cannot adopt this approach as our final model. However, considering possible reaction mechanisms using different ODE's and assessing their properties before going to the PDE version of the model, proved invaluable. First of all, integrating an ODE takes only a few seconds of computation time. So, after several seconds, the system adapts to the initial conditions and all of the initial transients are gone. So, a broad range of parameters and a wide range of different kinetic equations can be examined relatively quickly.

Although the ODE model can serve as an initial crude description, we need to take into account the spatial variation in protein concentration levels. In other words, we assume that every concentration is a function of spatial coordinates and time. Now, our equations have to be supplemented with appropriate diffusion terms. As prokaryotic cells lack active transport, diffusion ought to be the only mechanism of protein relocation. Considering the above discussion of the ODE the immediate choice of the model would be:

$$\frac{\partial So}{\partial t} = -k_1 \left(1 + \sigma_1 so^2\right) So + k_2 \left(so\right)\left(sp\right) + D_1 \nabla^2 So$$

$$\frac{\partial so}{\partial t} = k_1 \left(1 + \sigma_1 so^2\right) So - k_2 \left(so\right)\left(sp\right) + D_2 \nabla^2 so$$

$$\frac{\partial Sp}{\partial t} = k_3 sp - k_4 \left(Sp\right)\left(so\right) + D_2 \nabla^2 Sp \tag{3}$$

$$\frac{\partial sp}{\partial t} = -k_3 sp + k_4 \left(Sp\right)\left(so\right) + D_2 \nabla^2 sp$$

The notation is the same as above. The diffusion of Soj in the cytoplasm is assumed to occur with diffusion coefficient D_1, while all particles associated with the DNA are allowed to diffuse with diffusion coefficient D_2, chosen to be several orders of magnitude lower than D_1 as DNA binding is expected to decrease the mobility of the protein. Of course, the bacterial cell is three-dimensional and it would be most appropriate to model three-dimensional diffusion, meaning $\nabla^2 = \partial^2/\partial x^2 + \partial^2/\partial y^2 + \partial^2/\partial z^2$. Nevertheless, there are several reasons for adopting one-dimensional geometry ($\nabla^2 = \partial^2/\partial x^2$). First of all, modelling diffusion is to become the most expensive step in terms of CPU time: introducing diffusion in three dimensions will make the simulations extremely slow. On the other hand, we lack sufficient details on the organization and geometry of the interior of the bacterial cell and it is therefore desirable to adopt the simplest possible description.

Of course, we do not need to introduce separate variables for the concentration of species on the two nucleoids. However, we do need to introduce the nucleoids themselves. One simple way to accomplish this is simply to let k_1 depend on the spatial coordinate (x), and let it assume a large value in regions of space where the nucleoids are located. Indeed, this will imply that Soj is capable of switching to its DNA associated form (so) precisely in those regions. Now, Spo0J is always attached to the chromosome, where it undergoes condensation and decondensation. Therefore, the most obvious choice for modelling the chromosomes would be to set k_1 to zero at every position of the cell lacking DNA. Imposing zero flux conditions at the boundary of each nucleoid ensures that no protein particles can diffuse from the chromosome into the cytoplasm without undergoing active unbinding. In summary: we model the nucleoids by setting k_1 to:

$$k_1 = \begin{cases} K_1 & L/10 \le x \le 2L/5 \; or \; 3L/5 \le x \le 9L/10 \\ 0 & elsewhere \end{cases} \tag{4}$$

Where L is the length of the cell (approximately 4 μm). It is readily seen that the nucleoids are assumed to occupy most of the volume inside bacterial cell as was suggested by DAPI staining micrographs. At the same time we impose zero flux at the boundaries of the chromosomes ($x=L/10$, $x=2L/5$, $x=3L/5$ and $x=9L/10$).

Now, when the problem is reduced to differential equations it is of great interest to state something about the properties of the solutions. Unfortunately, such systems of coupled partial differential equations of second order with effectively cubic nonlinearities do not allow any satisfactory analytical treatment. In order to study their properties, one has to use numerical integration, which in this case does not pose

15

any particular difficulty. In our case the simplest explicit integration ("Euler forward"), turned out to be sufficient. The numerical procedure is:

$$So(t+dt,x) = So(t,x) + dt\left(-k_1\left(1+\sigma_1 so(t,x)^2\right)So(t,x)+\right.$$

$$\left.+k_2\left(so(t,x)\right)\left(sp(t,x)\right)+D_1\left(So(t,x+dx)-2So(t,x)+So(t,x-dx)\right)\frac{1}{dx^2}\right) \quad (5)$$

Time is discretized with a step dt which has to be sufficiently small in order to ensure stability of the numerical solution. The length of the cell was subdivided into 200 subvolumes of $dx=0.02$ μm each.

As stated above, an analytical solution of such complex systems of partial differential equations is usually impossible. Nevertheless, some analytical results can be acquired by means of linear stability analysis (or bifurcation theory). Here we briefly recapitulate how this treatment is conducted.

Assume that we have a system of (autonomous) partial differential equations of the form:

$$\frac{\partial \mathbf{f}}{\partial t} = \mathbf{F}(\mathbf{f}) + \mathbf{D}\nabla^2\mathbf{f} \quad (6)$$

In our case $\mathbf{f}$ is a vector of four elements, representing the concentration of the reacting species, $\mathbf{F}$ is some nonlinear vector-valued function, specifying the reaction rates and $\mathbf{D}$ is a matrix of diffusion coefficients (in our equations it is diagonal, but generally it need not be). Now, assume that we solve the equation $\mathbf{F}(\mathbf{f})=0$ and acquire a solution $\mathbf{f}^*$. Clearly, $\mathbf{f}(x,t)\equiv\mathbf{f}^*$ solves our PDE. Now, this solution is stationary and it does not depend on the spatial coordinates. If this solution would be stable, no dynamics would be observed in the system. However, if this homogeneous solution is unstable, we can expect a small perturbation to grow and finally lead the system into a state which potentially displays more interesting self-organizing properties (for example spatial and temporal periodicity). Let us assume that $\mathbf{f}^*$ is known. Now we substitute a solution of the form $\mathbf{f}^*+\delta\mathbf{f}$ and derive the equation governing the evolution of a (small) perturbation $\delta\mathbf{f}$.

$$\frac{\partial \delta\mathbf{f}}{\partial t} = \mathbf{F}\left(\mathbf{f}^*+\delta\mathbf{f}\right) + \mathbf{D}\nabla^2\delta\mathbf{f} = \mathbf{F}\left(\mathbf{f}^*\right) + \mathbf{J}\delta\mathbf{f} + O\left(\delta\mathbf{f}^2\right) + \mathbf{D}\nabla^2\delta\mathbf{f} \quad (7)$$

Where $\mathbf{J}$ is the Jacobian matrix of $\mathbf{F}$ at the "point" $\mathbf{f}^*$ ($\mathbf{J}_{ij}=\partial\mathbf{F}_i/\partial\mathbf{f}j \mid_{\mathbf{f}*}$). But taking into account that $\mathbf{F}(\mathbf{f}^*)=0$ by the definition of $\mathbf{f}^*$, and neglecting higher order terms, we arrive at the following equation, governing the evolution of $\delta\mathbf{f}$:

$$\frac{\partial \delta\mathbf{f}}{\partial t} = \left(\mathbf{J} + \mathbf{D}\nabla^2\right)\delta\mathbf{f} \quad (8)$$

Now, knowing that the eigenfunction of the Laplacian operator is sin we substitute a solution of the form $\mathbf{v}e^{\omega t}sin(qx)$, yielding:

$$\omega \mathbf{v} = \left(\mathbf{J} - q^2 \mathbf{D} \right) \mathbf{v} \qquad (9)$$

This means that the evolution of the perturbation is governed by a linearized eigenvalue equation. Now, assume that we solve this eigenvalue equation for ω as a function of q. This yields what is known as a dispersion relation, that is to say the relation between the wavelength and the frequency of a solution of the linearized differential equation. Such an analysis is customary in virtually all areas of nonlinear physics ranging from hydrodynamics to convection problems.

Finally, there are vital pieces of experimental evidence that have not yet been incorporated into our model. It was demonstrated that in the long filamentous cells, the Soj prefers to assemble at a nucleoid located close to a cell pole. Moreover, MinD, a protein which is predominantly found at the cell pole, is vital for the oscillations. From these facts it becomes evident that the cell pole plays an important role in the oscillatory dynamics. In fact it has been suggested that Soj exists in two distinct forms. Unpublished results by Löwe, mentioned above, seem to imply that whereas phosphorylated Soj (Soj-ATP) binds to the DNA, dephosphorylated Soj (Soj-ADP) is unable to assemble on the nucleoid and it has to undergo MinD promoted nucleotide exchange at the cell pole in order to regain its capability to assemble on the chromosome. In order to incorporate these facts into our model we suggest the following set of partial differential equations:

$$\frac{\partial So}{\partial t} = -k_1 \left(1 + \sigma_1 so^2 \right) So + k_5 so_{ADP} + D_1 \frac{\partial^2 So}{\partial x^2}$$

$$\frac{\partial so}{\partial t} = k_1 \left(1 + \sigma_1 so^2 \right) So - k_2 \left(so \right) \left(sp \right) + D_2 \frac{\partial^2 so}{\partial x^2}$$

$$\frac{\partial So_{ADP}}{\partial t} = k_2 \left(so \right) \left(sp \right) - k_6 So_{ADP} \left(1 + \sigma_2 so_{ADP}^2 \right) + D_1 \frac{\partial^2 So_{ADP}}{\partial x^2}$$

$$\frac{\partial so_{ADP}}{\partial t} = k_6 So_{ADP} \left(1 + \sigma_2 so_{ADP}^2 \right) - k_5 so_{ADP}$$

$$\frac{\partial Sp}{\partial t} = k_3 sp - k_4 \left(Sp \right) \left(so \right) + D_2 \frac{\partial^2 Sp}{\partial x^2}$$

$$\frac{\partial sp}{\partial t} = -k_3 sp + k_4 \left(Sp \right) \left(so \right) + D_2 \frac{\partial^2 sp}{\partial x^2}$$

$$(10)$$

Where So_{ADP} denotes the concentration of cytoplasmic Soj-ADP, so_{ADP} is the concentration of Soj associated to the polar membrane and undergoing nucleotide exchange, while So is now the concentration of cytoplasmic Soj-ATP. Consequently Soj is assumed to exist in four different forms. As it undergoes unbinding from the nucleoid, Soj-ATP is converted into Soj-ADP. Then, it has to diffuse to the cell pole where it undergoes cooperative association and acquires a phosphate group with the help of MinD. After unbinding from the membrane Soj-ATP is again able to rebind to the DNA. The fact that MinD is localized at the cell pole is incorporated into spatial variation of k_6 which controls the rate of Soj association with the membrane. We let k_6 assume its maximum at the pole, exponentially declining towards the middle of the cell.

This setup is in principle capable of explaining the preference of Soj to assemble close to the cell end.

Bacterial cell geometry
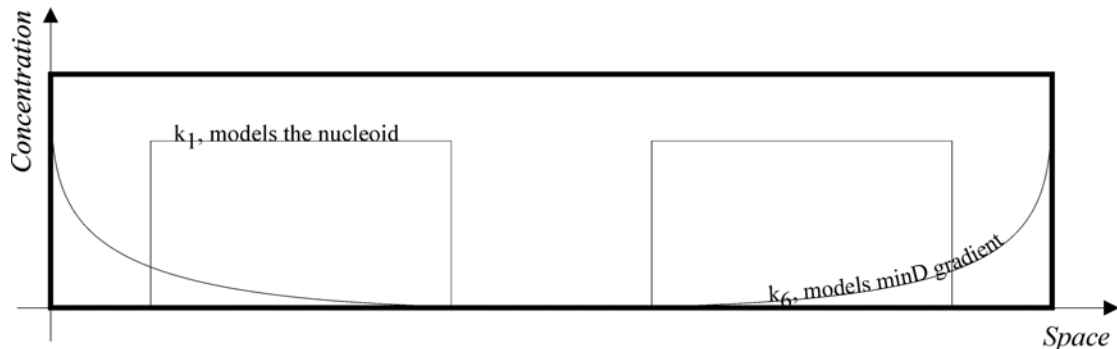
All the experimental data available on the Soj-Spo0J oscillation has underlined the profound stochasticity and unreliability of the observed oscillations. In some cells no oscillations at all were observed during one hour, while in others the frequency of Soj relocations was still very irregular. In principle, a PDE model can capture this feature if it exhibits chaotic dynamics. However, our numerical solutions gave us no reason to suspect that it did in our case. So, it seemed that the source of the irregularity in the frequency could be the stochastic nature of the chemical reactions. Of course, any model based on differential equations assumes that the number of particles is so large that using average concentrations is meaningful. Western-blot experiments demonstrated that the average copy number of Spo0J was approximately 1500 units per cell. When the number of reactants becomes this low it is more appropriate to model the number of reacting particles at each site of the bacterial cell, rather than their average concentrations. We hope that by doing so we will be able to explain the erratic behaviour observed in the Soj-Spo0J system.

The most straightforward way of setting up a Monte-Carlo simulation, modelling the number of discrete particles, would be to translate all the reaction intensities and diffusion intensities into the corresponding reaction and diffusion probabilities, sample a random number from a uniform distribution between *0* and *1,* and execute either a reaction or a diffusion transition if the corresponding probability turns out to be greater than the number sampled. Let us describe the algorithm in more detail.

First we discretize space into *n* compartments of equal length. In our case, if the cell length was 4 μm, we choose *n=200*. Making the length of every compartment even shorter has two drawbacks. On one hand, the computation time increases and on the other hand the size of the compartment becomes comparable to the size of the proteins it is supposed to contain, which is inappropriate. Therefore, a 0.02 μm subvolume seemed to suit our needs.

Now, the initial conditions have to be specified, that is to say, one must distribute the protein molecules among the compartments. It is just like giving the initial conditions of the PDE.

After this has been done we need to consider all possible transitions taking place inside the reaction chamber (which is the bacterial cell in our case). It is convenient to

represent the state of the system with a state vector, specifying the number of each of the reacting species. Of course, as the spatial variation of the concentration is taken into account we will need one such vector for every subvolume of the discretized reaction vessel.

Space discretization
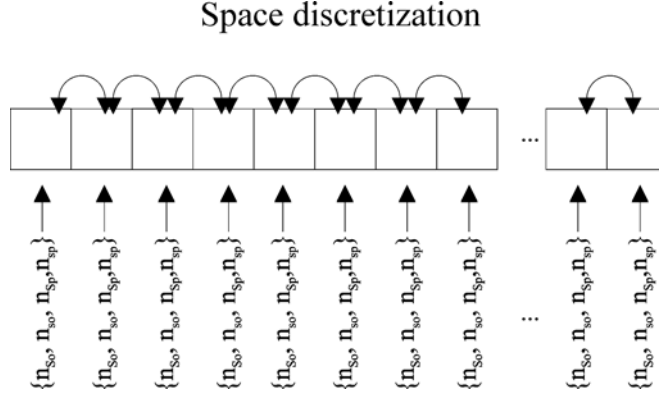
If we restrict out attention to one such compartment, the possible transitions due to reactions are:

$$\{n_{So}, n_{so}, n_{Sp}, n_{sp}\} \rightarrow \{n_{So} - 1, n_{so} + 1, n_{Sp}, n_{sp}\}$$

$$\{n_{So}, n_{so}, n_{Sp}, n_{sp}\} \rightarrow \{n_{So} + 1, n_{so} - 1, n_{Sp}, n_{sp}\}$$

$$\{n_{So}, n_{so}, n_{Sp}, n_{sp}\} \rightarrow \{n_{So}, n_{so}, n_{Sp} - 1, n_{sp} + 1\}$$

$$\{n_{So}, n_{so}, n_{Sp}, n_{sp}\} \rightarrow \{n_{So}, n_{so}, n_{Sp} + 1, n_{sp} - 1\}$$

Where n_S denotes the number of protein S molecules in the given compartment. Clearly, the total number of protein particles will be conserved, as the number of molecules is always the same before and after each transition. Note that each transition corresponds to one of the terms of the above PDE in an obvious way. Assume that the length of every compartment is l. It can be shown that the probability of the first transition (corresponding to the k_1-term) of the PDE occurring during a time interval Δt is given by $\Delta t k_1 (1 + \sigma_1 (n_{so})^2 / l^2) n_{So}$. The quantity $k_1 (1 + \sigma_1 (n_{so})^2 / l^2) n_{So}$ (the probability per time unit) is termed the intensity (I). The other reaction transition probabilities can be calculated in the same fashion.

Any molecule can relocate to the neighbouring subvolume (either to the left or to the right). Similarly, another molecule can rather diffuse into the current subvolume from one of the neighbouring compartments. It can be demonstrated that if the diffusion coefficient of a protein molecule is D, then the probability of a molecule leaving the compartment of length l during a period of time Δt is given by $D\Delta t / l^2$.

In summary, the algorithm we use for the simulation of the stochastic system is:

- Initialization:
    - Distribute the particles among the subvolumes
- Iteration:
    - Loop through the subvolumes
        - Loop through all possible transitions (due to reaction and due to diffusion)

- Sample a number $0 \leq r \leq 1$ from a uniform distribution
- Calculate the intensity of the current transition I
- Execute the transition if $I\Delta t > r$

It is important to note that whenever the intensity is converted into a probability one multiplies it with the quantity Δt. Clearly, if Δt is not sufficiently small and some of the probabilities exceed *0.5* the algorithm becomes unstable. On the other hand, if Δt is chosen to be so small that the highest transition probabilities become tiny, the algorithm will spend most of the time rejecting transitions. Consequently, we have a trade-off between stability and efficiency, just as is the case with PDE integration.

One hypothetical way around this problem would be to adopt the so called Gillespie's algorithm. The main idea behind this procedure is to calculate event times rather than their probabilities. It can be shown that, if the intensity of a transition is I, then the time at which it occurs is exponentially distributed according to $P(t) = Ie^{-tI}$. Therefore, an alternative to the algorithm above would be:

- Initialization:
  - Distribute the particles among the subvolumes
    - Loop through all the subvolumes and determine the total event intensity (as the sum of intensities of individual transitions)
      - Sample time for the next event to take place in the current compartment.
- Iteration
  - Search thorough the subvolumes and determine the one in which the earliest event is to take place
  - Determine the transition to execute (the probability of executing a given transition is proportional to its intensity)
  - Execute the transition
  - Recalculate the intensities
    - In the current subvolume if a reaction took place
    - In both the current and neighbouring subvolumes if diffusion took place
  - Increment the event time for the compartments where transitions occurred

The benefit of Gillespie's algorithm lies in the fact that it never rejects any transitions. It merely calculates the time at which the given transition is to take place and if there are any events prior to that time point, it executes them first.

However, each step of this algorithm requires a search through all of the subvolumes in order to determine the one where the earliest event is to take place. After running the simulations several times using both Gillespie's algorithm, and our simple procedure, outlined above, it turned out that the comparatively small decrease in computation time is not worth the effort of adopting the more sophisticated numerical procedure. So, the first, simple algorithm, was adopted.

Results:

Our first attempt was the following model:

$$\frac{\partial So}{\partial t} = -k_1 (So)(so) + k_2 (sp)(so)$$

$$\frac{\partial so}{\partial t} = k_1 (So)(so) - k_2 (sp)(so)$$

$$\frac{\partial Sp}{\partial t} = k_3 sp - k_4 (so)(Sp)(sp) \qquad (11)$$

$$\frac{\partial sp}{\partial t} = -k_3 sp + k_4 (so)(Sp)(sp)$$

The notations are the same as in the methods section above. The binding of Soj to DNA is assumed to occur cooperatively (Hill coefficient equals one). The condensation of Spo0J is cooperative as well and it is promoted by Soj, associated with the nucleoid. This model does not take into account the presence of the second nucleoid. If it is to produce oscillations, Soj will relocate from nucleoid to cytoplasm and back, rather than from one nucleoid to the adjacent one.

The results of the corresponding simulation using time step $\Delta t=0.01$ are given in figure (3). Clearly, the model is capable of producing oscillations, but they die out after a sufficiently long time. This implies the presence of a stable focus. If the focus is not destabilized for any parameter values, the model is inappropriate.

It is, however, not unreasonable to suppose that introducing a second nucleoid, without changing the parameters might yield a stable limit cycle. The corresponding set of ordinary differential equations is:

$$\frac{\partial So}{\partial t} = -k_1 (So)(so_1) - k_1 (So)(so_2) + k_2 (sp_1)(so_1) + k_2 (sp_2)(so_2)$$

$$\frac{\partial so_1}{\partial t} = k_1 (So)(so_1) - k_2 (sp_1)(so_1)$$

$$\frac{\partial so_2}{\partial t} = k_1 (So)(so_2) - k_2 (sp_2)(so_2) \qquad (12)$$

$$\frac{\partial Sp_1}{\partial t} = k_3 sp_1 - k_4 (so_1)(Sp_1)(sp_1) \qquad \frac{\partial sp_1}{\partial t} = -k_3 sp_1 + k_4 (so_1)(Sp_1)(sp_1)$$

$$\frac{\partial Sp_2}{\partial t} = k_3 sp_2 - k_4 (so_2)(Sp_2)(sp_2) \qquad \frac{\partial sp_2}{\partial t} = -k_3 sp_2 + k_4 (so_2)(Sp_2)(sp_2)$$

As is seen from these equations, all of the dynamics is exactly the same as in the previous case, only now there are three distinct Soj concentrations (in the cytoplasm, and on the two nucleoids) and four different Spo0J concentrations (in its condensed and uncondensed form on each nucleoid). However, all the kinetic assumptions regarding cooperativity and stoichiometry are kept the same. The results of the corresponding simulation (with some minor modifications which are skipped) are given in figure (4). Now the oscillations are far more stable. Basically, we have coupled two unstable oscillators and this coupling stabilized the limit cycle to some extent. Examining when this occurs in a more general context would constitute an

interesting research topic. However, longer simulations turned out to indicate that the amplitude gradually decreased even in this case.

After trying a wide range of parameters and several other models, similar to equation (12), we came to the conclusion that such a simple and straightforward phenomenology is not sufficient for capturing the oscillatory behaviour. The reason that we envisaged for this was the following. In the course of every Soj relocation, this protein first assembles on one chromosome and causes Spo0J to condense. Condensed Spo0J expels the Soj back into the cytoplasm. But Soj is capable of dissociating as soon as it assembles on the chromosome. Therefore, at some point the rate of association precisely balances the rate of dissociation and the system relaxes to a stationary steady state without any oscillations occurring. A solution to this problem would be to let the concentration of the condensed Spo0J at which Soj starts to dissociate from the nucleoid be somewhat higher than the Spo0J concentration at which Soj starts to bind to the DNA. Between these values, no appreciable dynamics of Soj should occur. In other words, hysteresis must be introduced. A radical way of achieving this would be to add the rather artificial and somewhat unphysical dynamics:

$$\frac{\partial So}{\partial t} = -k_1(So)(so_1) - k_1(So)(so_2) + H(sp_1)k_2(so_1)(sp_1) + H(sp_2)k_2(so_2)(sp_2)$$

$$\frac{\partial so_1}{\partial t} = k_1(So)(so_1) - H(sp_1)k_2(so_1)(sp_1)$$

$$\frac{\partial so_2}{\partial t} = k_1(So)(so_2) - H(sp_2)k_2(so_2)(sp_2)$$

$$\frac{\partial Sp_1}{\partial t} = k_3sp_1 - k_4(Sp_1)(so_1)(sp_1) \quad \frac{\partial sp_1}{\partial t} = -k_3sp_1 + k_4(Sp_1)(so_1)(sp_1)$$

$$\frac{\partial Sp_2}{\partial t} = k_3sp_2 - k_4(Sp_2)(so_2)(sp_2) \quad \frac{\partial sp_2}{\partial t} = -k_3sp_2 + k_4(Sp_2)(so_2)(sp_2)$$

$$(13)$$

Where H signifies a relay-function:

$$H(z) = \begin{cases} h(z-\delta) & if \quad \dot{z} > 0 \\ h(z-\varepsilon) & if \quad \dot{z} < 0 \end{cases} \quad (14)$$

$$\varepsilon < \delta$$

Where z-dot is the time derivative of z, and h on the left hand side signifies the Heaviside step function.

This model was the first one among the ones constructed that did display stable oscillations. The results of the numerical simulation are given in figure (5). Interestingly, these equations exhibited rather varying behaviour in different parameter ranges.

Although, the hysteresis mechanism seemed to be appropriate, it is not clear how to introduce it into a biologically motivated model. Clearly, introducing it in this straightforward fashion is somewhat unphysical. As was shown in the methods

section, the easiest way of accomplishing this would be to introduce quadratic cooperativity. Then, if the bifurcation diagram would look like a cubic polynomial, folding back on itself, the model would be expected to exhibit hysteresis.

As our first suggestion we used:

$$\frac{\partial So}{\partial t} = -k_1 (So)(so_1) - k_1 (So)(so_2) + k_2 (sp_1)(so_1) + k_2 (sp_2)(so_2)$$

$$\frac{\partial so_1}{\partial t} = k_1 (So)(so_1) - k_2 (sp_1)(so_1)$$

$$\frac{\partial so_2}{\partial t} = k_1 (So)(so_2) - k_2 (sp_2)(so_2)$$

$$\frac{\partial Sp_1}{\partial t} = -k_3 (so_1)(Sp_1)(sp_1) + k_4 (Sp_1)^2 (sp_1) \qquad (15)$$

$$\frac{\partial sp_1}{\partial t} = k_3 (so_1)(Sp_1)(sp_1) - k_4 (Sp_1)^2 (sp_1)$$

$$\frac{\partial Sp_2}{\partial t} = -k_3 (so_2)(Sp_2)(sp_2) + k_4 (Sp_2)^2 (sp_2)$$

$$\frac{\partial sp_2}{\partial t} = k_3 (so_2)(Sp_2)(sp_2) - k_4 (Sp_2)^2 (sp_2)$$

The results of the corresponding simulations are given in figure (6). The main feature yielding the oscillations is quadratic cooperativity in the decondensation of Spo0J. The main virtue of this model is that it is able to exhibit stable oscillations and unlike the previous case, the hysteresis is derived from the kinetic assumptions rather than assumed *a priori*. However, the nature of Spo0J condensation-decondensation is poorly known. Therefore it would be a benefit to reduce the number of assumptions regarding this step. Furthermore, experimental work suggested that the binding of Soj rather than Spo0J decondensation proceeds in a highly cooperative fashion. Therefore, we aimed to find the simplest possible model with cooperativity in Soj association. After several attempts we settled on the following version of the kinetic rate equations:

$$\frac{\partial So}{\partial t} = -k_1 \left(1 + \sigma_1 (so_1)^2\right)(So) - k_1 \left(1 + \sigma_1 (so_2)^2\right)(So) + k_2 (so_1)(sp_1) + k_2 (so_2)(sp_2)$$

$$\frac{\partial so_1}{\partial t} = k_1 \left(1 + \sigma_1 (so_1)^2\right)(So) - k_2 (so_1)(sp_1)$$

$$\frac{\partial so_2}{\partial t} = k_1 \left(1 + \sigma_1 (so_2)^2\right)(So) - k_2 (so_2)(sp_2) \qquad (16)$$

$$\frac{\partial Sp_1}{\partial t} = k_3 sp_1 - k_4 (Sp_1)(so_1) \qquad \frac{\partial sp_1}{\partial t} = -k_3 sp_1 + k_4 (Sp_1)(so_1)$$

$$\frac{\partial Sp_2}{\partial t} = k_3 sp_2 - k_4 (Sp_2)(so_2) \qquad \frac{\partial sp_2}{\partial t} = -k_3 sp_2 + k_4 (Sp_2)(so_2)$$

The simulation results are depicted in figure (7). This model is probably the absolutely simplest rationalization of experimentally demonstrated facts. Only one

term is cooperative, namely the rate of Soj assembly on the nucleoid, as was suggested in the experimental papers.

When converting the ODE into a PDE, the equations have to be supplemented with appropriate diffusion terms, as was shown in the methods section.
First let us consider the simple case given by:

$$\frac{\partial So}{\partial t} = -k_1\left(1+\sigma_1 so^2\right)So + k_2\left(so\right)\left(sp\right) + D_1\nabla^2 So$$

$$\frac{\partial so}{\partial t} = k_1\left(1+\sigma_1 so^2\right)So - k_2\left(so\right)\left(sp\right) + D_2\nabla^2 so$$

$$\frac{\partial Sp}{\partial t} = k_3 sp - k_4\left(Sp\right)\left(so\right) + D_2\nabla^2 Sp \tag{17}$$

$$\frac{\partial sp}{\partial t} = -k_3 sp + k_4\left(Sp\right)\left(so\right) + D_2\nabla^2 sp$$

The results of the numerical integration are shown in figure (8). Clearly, Soj regularly relocates from one nucleoid to the adjacent one. The oscillation resembles a square pulse with a small characteristic cusp.

Clearly, the equations above are not accounting for the MinD-promoted nucleotide exchange, occurring at the cell pole. However, one of the Spo0J mutants, isolated by means of site directed mutagenesis apparently did not require the cell pole-interactions in order to rebind to the adjacent nucleoid after dissociating from the chromosome. Therefore, this simple set of equations can serve as an appropriate model of the Soj dynamics in this mutant strain.

Including nucleoid-polar shuttling into our model yields equation (10). The aim is to faithfully model the Soj relocations in the wild type cells. The results of the corresponding numerical simulation are depicted on figure (9). The oscillations are still very similar to the ones, obtained in the previous case. The amplitude is somewhat smaller, reflecting the fact that a greater fraction of Soj remains in the cytoplasm, as a result of needing to undergo MinD promoted nucleotide exchange.

Let us perform linear stability analysis of equation (17). When this is done we will be in position to say something about the emergence of spatiotemporal self-organization. Furthermore, this treatment allows an extraction of the characteristic wavelength.

The equations, considered are:

$$\frac{\partial So}{\partial t} = -k_1\left(1+\sigma_1 so^2\right)So + k_2\left(so\right)\left(sp\right) + D_1\nabla^2 So$$

$$\frac{\partial so}{\partial t} = k_1\left(1+\sigma_1 so^2\right)So - k_2\left(so\right)\left(sp\right) + D_2\nabla^2 so$$

$$\frac{\partial Sp}{\partial t} = k_3 sp - k_4\left(Sp\right)\left(so\right) + D_2\nabla^2 Sp \tag{18}$$

$$\frac{\partial sp}{\partial t} = -k_3 sp + k_4\left(Sp\right)\left(so\right) + D_2\nabla^2 sp$$

In order to make things simple, we drop the spatial dependence of k_1. Else, the treatment becomes too complicated.

We start by setting left hand side of the equation to zero, and dropping the Laplacian terms. Then, the set of algebraic equations can be solved in a computer aided fashion. It turned out that this set of equations admitted three solutions for the kinetic parameters adopted in the numerical simulations. One of the solutions was complex, another one was negative and, finally, the third one was real. This solution of the algebraic equation is also a (physical) homogeneous stationary solution of the PDE. Now, the equations have to be linearized around this "stationary point". The Jacobian matrix is easily obtained by computing partial derivatives of the left hand side.

$$\mathbf{J} = \begin{bmatrix} -k_1\left(1+\sigma_1 so^2\right) & -2k_1\sigma_1(so)(So)+k_2 sp & 0 & k_2 so \\ k_1\left(1+\sigma_1 so^2\right) & 2k_1\sigma_1(so)(So)+k_2 sp & 0 & -k_2 so \\ 0 & k_4 Sp & -k_4 so & k_3 \\ 0 & -k_4 Sp & k_4 so & -k_3 \end{bmatrix} \quad (19)$$

Of course, numerical values of So, so, Sp and sp have to be substituted into the above expression.

Now, we are in a position to determine the dispersion relation. By evaluating the eigenvalue of the matrix $\mathbf{J}\text{-}\mathbf{D}q^2$ (the notation is the same as in the methods section), we compute the amplitude of every Fourier mode in the expansion of the perturbation. The results are depicted in figure (10).

Importantly, we see that the real part of the eigenvalue is indeed positive for certain values of q. This implies the presence of an instability. Therefore, the mechanism behind spatio-temporal pattern formation in our system is related to the so called Turing (Hopf) instability.

Furthermore, the value of $q=q_{max}$, corresponding to the eigenvalue with the largest real part corresponds to the characteristic wavelength: $\lambda=2\pi/q$. Reading off q_{max} from figure (10) yields the value $\lambda_{char}=6$ μm.

The equations above were integrated numerically and the space-time plot showed the emergence of propagating waves with a characteristic wavelength, approximately equal to the one obtained by linear stability analysis.

As was explained in the methods section, in this case the stochastic Monte-Carlo simulation is needed in order to capture the fragility of the oscillations, observed in the experiments. Our main claim is that the irregularity in the frequency of the Soj relocations can be explained in terms of the stochastic nature of the chemical reactions, without introducing any additional sources of noise.

It turned out that the model still had to be modified somewhat in order to capture all the aspects of the experimental data. In particular, it proved impossible to make the model robust with respect to changes in the total protein amounts. Long filamentous

Spo0J mutants containing roughly three times more Soj than the wild type failed to exhibit any dynamics, contrary to the experimental data. The modified PDE now looks like:

$$\frac{\partial So}{\partial t} = -k_1\left(1+\sigma_1 so^2\right)So + k_2\left(so\right)\left(1+\sigma_3 so\right)\left(sp\right) + D_1\nabla^2 So$$

$$\frac{\partial so}{\partial t} = k_1\left(1+\sigma_1 so^2\right)So - k_2\left(so\right)\left(1+\sigma_3 so\right)\left(sp\right) + D_2\nabla^2 so$$

$$\frac{\partial Sp}{\partial t} = k_3 sp - k_4\left(Sp\right)\left(so\right) + D_2\nabla^2 Sp$$

$$\frac{\partial sp}{\partial t} = -k_3 sp + k_4\left(Sp\right)\left(so\right) + D_2\nabla^2 sp$$

(20)

Now the k_2 term includes a $\sigma_3(so)$ factor, basically implying that Soj forms dimers before dissociating from the nucleoid. Structural data on ParA family proteins supports this assumption. Moreover, cooperative unbinding was suggested by one of the experimental papers (Marston *et al.*, 1999).

The details of converting this set of PDEs into the corresponding stochastic model are given in the methods section.

First, we omit the MinD promoted nucleotide exchange at the cell pole. As mentioned above, this model is meant to reproduce the dynamics of one of the Spo0J mutant which we believe lacks nucleoid-polar shuttling.

The results of the corresponding Monte-Carlo simulation are depicted in figure (11). Clearly, Soj undergoes rather erratic, irregular jumps from one nucleoid to the other. Sometimes it dwells on one nucleoid without relocating during some 15-20 minutes, and in other cases the relocation is accomplished in only 5-6 minute time.

Now, we introduce the cell pole and try to capture the dynamics in the wild type. The corresponding PDE model is given by equation (10). The k_2 term is modified in the same way as in the previous example. The results of the simulation are given in figure (12). Now, the probability of relocation from one nucleoid to the proximal one is much lower. Occasionally, all the Soj assembles on one chromosome without any jumps occurring during 30-60 minutes. This fact is in good agreement with the experimental data. Indeed, in many time lapse experiments some cells did not exhibit any dynamics at all during one hour's observation time. So, the introduction of the cell pole interaction effectively increases the period and makes the oscillations more erratic, in accordance with the experimental data.

As the length of the cell is a simple parameter of our model, we are clearly in a position to increase it and examine the dynamics in the case of long *ftsZ* filaments. As mentioned in the experimental background section, these cells lack the protein, marking the mid-cell during cell division. Therefore, they do not divide, while DNA replication and the synthesis of all the cellular components proceeds at approximately the same rate as in the wild type. In the corresponding simulation we increase the cell length by a factor of four. The number of nucleoids and the total protein amounts are changed accordingly. In particular, the amount of MinD ought to increase by the same

factor. When implementing the stochastic algorithm we modelled the MinD profile as a step function rather then an exponential decay. By increasing the length of the step by a factor of four we take into account the increase in the total MinD amount. This feature turned out to be critical for capturing the qualitative aspects of the dynamics in the *ftsZ* filaments. The results of the corresponding simulation are given in figure (13). Clearly, all the Soj assembles on a single cell pole proximal nucleoid, in full accordance with the experimental data. Clearly, as the cell length increases, the probability for an individual molecule to diffuse all the way to the other pole, undergo nucleotide exchange and assemble on the nucleoid at the opposite cell end must decrease.

However, when the dependence on the cell pole is suppressed by a Spo0J mutation, the dynamics was expected to resume. The results of the numerical simulation are depicted in figure (14). Now, we use four-fold increases: the cell length, the total protein amounts, and the number of nucleoids. The Soj oscillations persist and their frequency is similar to that of the normal length Spo0J mutant. This observation is also in full agreement with the experimental results.

Finally, a mutant, unable to undergo nucleotide exchange at the cell pole was described in one of the experimental papers (Quisel *et al.*, 1999). In our model this corresponds to dropping the k_5 term of equation (10). Now Soj assembles in narrow bands close to the cell pole. This very behaviour was observed in the experiments.

Conclusions

In this work we have shown that an accurate description of protein relocation patterns can be obtained by means of numerical modelling, using only the most basic assumptions of the kinetics, derived from experimental data.

Most of the experimental observations are plausibly reproduced by our models. The system is indeed capable of producing oscillations, the behaviour in the long filaments is captured appropriately in the corresponding simulations and the effects of Spo0J mutation are accounted for in the modified version of the model.

Yet, several experimentally determined features have still not been incorporated into our description. For example, Spo0J was shown to assemble into tighter foci than Soj did. This was not the case in our numerical experiments. This is probably a consequence of the fact that we did not explicitly model the binding sites at the nucleoid. Rather, both chromosomes were represented as two distinct impenetrable "compartments", containing Spo0J. Moreover, the condensation of Spo0J foci was shown to be accompanied by DNA reorganization. As the nature of this process is poorly understood, we chose to adopt the most basic assumption of first order kinetics. Therefore, some details of Soj and Spo0J interactions with the nucleoid were not reproduced appropriately.

At this point we would like to stress that our main aim was to put forward the simplest possible qualitative description of the dynamics. This work suggests that the emergence of Soj oscillations in *B. subtilis* (and possibly many other related bacterial species) relies on the high degree of cooperativity in the binding of Soj to the nucleoid. This self enhancing association results in hysteresis, destabilizing an otherwise stable

steady state. Of course, determining the precise values of all the kinetic parameters (for example by means of stopped flow experiments) could shed additional light on the nature of the process. As no such measurements have been done, we were forced to manually adjust the kinetic constants so that the model reproduced the observed dynamics. However, our results were robust with respect to large changes of all of the parameters, varying total protein amounts and changes of the cell geometry.

Although our modelling managed to reproduce the dynamics, it did not shed much light on the function of the Soj oscillations. Here, we suggest two possible explanations. It is known that Spo0J condensation is accompanied by DNA reorganization. As the foci assemble, distinct strands are probably brought together and interlocked by means of interactions between the distinct Spo0J molecules bound to different regions of the chromosome. Repeated condensations and decondensations might allow the nucleoid to assume the most favourable configuration, tightening the DNA patch before the initiation of chromosome partitioning between the two daughter cells. Another possibility is that the oscillations create a time average minimum (or maximum) of some protein at some particular position of the cell, serving as a topological marker, as in the case of *min* system, mentioned in the background section.

In any case, our modelling provides an accurate qualitative explanation of the emergence of spatio-temporal self-organization in our particular biological system.

A number of possible extensions of the results of this work can be outlined. Unfortunately, we did not have time to examine these issues in any detail.

First of all, the generality of the model can be assessed. Our initial investigation, recapitulated in the methods section, showed that there only exist a very limited number of ordinary differential equations with four interacting species, conserving the total amounts of the interacting components and reasonable kinetic assumptions, exhibiting a stable limit cycle. It seems possible, that all such systems could be constructed in a rather straightforward manner and their capability of producing oscillations could be assessed. Furthermore it is not impossible that there would be a way of discriminating between the different models by means of some simple procedure (for example by examining the dependence of the period on the total amounts of different species). This could in principle provide a way of classifying the different chemical oscillative systems and moreover the determination of the kinetic equations from very limited experimental data could then be achieved.

Another interesting observation of this work is the emergence of oscillations after introducing hysteresis into the system. Now, the question arises: what is the precise requirement for destabilization of a stable state after introducing a hysteresis term (for example in the same fashion as was done in (13)). This question is not particularly relevant to the current work, but it could be interesting, for example, in the context of system control, where hysteresis is a common form of nonlinearity. The main aim in this branch of applied mathematics is to keep the system at the steady state by designing an appropriate feedback. So, the influence of hysteresis on the emergence of oscillatory behaviour could be of great interest in this field.

Another issue, worth investigating, is the details of the kinetic assumptions of our model. From the structural analysis of ParA family proteins it seems plausible that Soj polymerises, upon associating to the nucleoid. The details of this process are unknown. However let us for a moment consider the problems one is confronted with when trying to put forward plausible assumptions about the kinetics. Suppose that two Soj molecules would be capable of associating and forming a dimer, which in its turn could bind yet another Soj particle and form a trimer. This process could continue until all of the Soj would be found in the polymerised form. It seems reasonable to assume that the rate at which the multimer containing n Soj particles (So_n) is produced is:

$$\frac{\partial So_n}{\partial t} = k \sum_{i+j=n} (So_i)(So_j)$$

where k is the rate constant for association between the different Soj polymers. This is assumed to be independent of the number of monomers comprising the interacting polymers. Following this argument, it should be possible to find the rate at which the polymerisation proceeds as a function of the concentration of monomers. This effective rate could then be incorporated into our model (basically, by modifying k_1), in order to hopefully yield a better description of the dynamics.

The stability analysis of our PDE also exhibited some rather unexpected properties. It is customary that the frequency of the oscillation is determined by the imaginary part of the eigenvalue with the largest real part. Although some values of the wavenumber q did yield a complex eigenvalue of the linearized system with a positive real part (implying the presence of the so called Hopf bifurcation, as mentioned above), the eigenvalue with the largest real part was real. This does not contradict the conclusions of the linear stability analysis. Such a treatment is indeed nothing more than a rule of thumb. This observation implies that the linear analysis is insufficient for explaining the basic oscillatory features of the solution and higher order approximations, accounting for the nonlinearity are necessary. Hence, the PDE model is worth investigating further.

The main aim of the stochastic simulations was to reproduce the irregularity of the frequency observed in experiments. Our PDE models on the other hand did not display any irregularity at all. The relocations occurred with the same period, suggesting that the source of the stochasticity is not the chaotic behaviour of the corresponding PDE model. Yet, it can be shown that, if the total amounts of the reacting species become sufficiently high, the dynamics of the average concentrations in the Monte-Carlo model will be precisely the same as in the PDE version. In our case we had an approximate estimate of the total protein amounts in a *B. subtilis* cell. By means of western blotting it was determined that the approximate copy number of Spo0J molecules per cell was 1500. This is a comparatively large number. Therefore, it was expected that the irregularity of the oscillation would be hard to reproduce. However, when Soj assembles on one of the chromosomes, and is ready to relocate to the proximal one, the system finds itself in an unstable state. Therefore, Soj might either relocate or reassemble at the same nucleoid shortly after dissociation, meaning that stochasticity is retained at high concentration levels. Interestingly, the oscillations became more erratic as the order of magnitude of the kinetic parameters controlling Spo0J condensation and decondensation was made similar to the order of the

magnitude of the parameters controlling the dynamics of Soj. This could in principle be a general feature: the influence of noise was greater when the different timescales of the system become similar. This issue is also worth further investigation.

Finally, details of the inner structure of a bacterial cell, data on the intracellular geometry and nucleoid organization are all very scarce. All these additional features could in principle be incorporated into the model, hopefully providing a better description of the Soj oscillations.

References

Autret, S. & Errington, J. A role for division-site-selection protein MinD in regulation of internucleoid jumping of Soj (ParA) protein in *Bacillus subtilis*. *Mol. Microb.* **47**(1)**,** 159-169 (2003)

Autret, S., Nair, R. & Errington, J. Genetic analysis of the chromosome segregation protein Spo0J of *Bacillus subtilis*: evidence for separate domains involved in DNA binding and interactions with Soj protein. *Mol. Microb.* **41**(3)**,** 743-755 (2001)

B. P. Belousov (1958). Sb. Ref. Radiats. Med.Medgiz, Moscow, 1959, p 145.
The early history of the BZ reaction is described in: A. T. Winfree (1984). *J. Chem. Educ.*, 61, 661.

Cervin A. M., Spiegelman B. G., Raether B., Ohlsen K., Perego M. & Hoch A. J. A negative regulator linking chromosome segregation to developmental transcription in *Bacillus subtilis*. *Mol. Microb.* **29**(1)**,** 85-95 (1998)

Chi-Hong Lin, D. & Grossman, D. A. Identification and Characterization of a Bacterial Chromosome Partitioning Site. *Cell* **92,** 675-685 (1998)

Chi-Hong Lin D., Levin A. L. & Grossman D. A. Bipolar localization of a chromosome partition protein in *Bacillus subtilis*. *Proc. Natl. Acad. Sci. USA* **94,** 4721-4726 (1997)

Glaser, P., Sharpe E. M., Raether, B., Perego, M., Olsen, K. & Errington, J. Dynamic, mitotic-like behaviour of a bacterial protein required for accurate chromosome partitioning. *Genes & Dev.* **11,** 1160-1168 (1997)

Howard, M. A Mechanism for Polar Protein Localization in Bacteria. *J. Mol. Biol.* **335,** 655-663 (2004)

Howard, M. & Rutenberg D. A. Pattern Formation inside Bacteria: Fluctuations due to Low Copy Number of Proteins. *Phys. Rev. Lett.* **90**(12)**,** 128102 (2003)

Howard, M., Rutenberg, D. & de Vet, S. Dynamic Compartmentalization of Bacteria: Accurate Division in *E. coli*. *Phys. Rev. Lett.* **87**(27), 278102 (2001)

Hunding, A., Ebersbach, G. & Gerdes, K. A Mechanism for ParB-dependent Waves of ParA, a Protein Related to DNA Segregation during Cell Division in Prokaryotes. *J. Mol. Biol.* **329,** 35-43 (2003)

Ireton, K., Gunther, W. N. & Grossman D. A. *spo0J* Is Required for Normal Chromosome Segregation as well as the Initiation of Sporulation in *Bacillus subtilis*. *J. Bacteriol.* **176**(17)**,** 5320-5329 (1994)

Leonard A. T., Butler G. P. and Löwe J. Structural analysis of the chromosome segregation pretein Spo0J from *Thermus thermophilus*. *Mol. Microb.* **53**(2)**,** 419-432 (2004)

Marston, L. A. & Errington, J. Dynamic Movement of the ParA-like Soj protein of *B.subtilis* and Its Dual Role in Nucleoid Organization and Developmental Regulation. *Mol. Cell* **4,** 673-682 (1999)

G. Nicolis and Ilya Prigogine *Self-Organization in Non-Equilibrium Systems*, 1977, Wiley, ISBN 0471024015

Ogura Y., Ogasawara N., Harry J. E. & Moriya S. Increasing the Ratio of Soj to Spo0J Promotes Replicaton Initiation in *Bacillus subtilis*. *J. Bacteriol.* **185**(21)**,** 6316-6324 (2003)

Pogliano J., Sharp D. M. & Pogliano K. Partitioning of Chromosomal DNA during Establishment of Cellular Asymmetry in *Bacillus subtilis*. *J. Bacteriol.* **184**(6)**,** 1743-1749 (2002)

Quisel, J. Q. & Chi-Hong Lin, D. Control of Development by Altered Localization of a Transcription Factor in *B. subtilis*. *Mol. Cell* **4,** 665-672 (1999)

Quisel D. J. & Grossman D. A. Control of Sporulation Gene Expression in *Bacillus subtilis* by the Chromosome Partitioning Proteins Soj (ParA) and Spo0J (ParB). *J. Bacteriol.* **182**(12)**,** 3446-3415 (2000)

Van Ooij, C. & Losick R. Subcellular Localization of a Small Sporulation Protein in *Bacillus subtilis*. *J. Bacteriol.* **185**(4)**,** 1391-1398 (2003)

Walker J. E., Saraste M., Runswick M. J. & Gay N. J. Distantly related sequences in the alpha- and beta-subunits of ATP synthetase, myosin, kinases and other ATP-requiring enzymes and a common nucleotide binding fold. *EMBO J.* **1**, 945-951 (1982)

Wu J. L. & Errington J. A large dispersed chromosomal region required for chromosome segregation in sporulating cells of *Bacillus subtilis*. *EMBO J.* **21**(15)**,** 4001-4011 (2002)

Wu J. L. & Errington J. RecA and the Soj-Spo0J system combine to effect polar hromosome segregation in sporulating *Bacillus subtilis*. *Mol. Microb.* **49**(6), 1463-1475 (2003)

Yamaichi Y. & Niki H. Active segregation by the *Bacillus subtilis* partitioning system in *Escherichia coli*. *Proc. Natl. Acad. Sci. USA* **97**(26), 14656-14661 (2000)

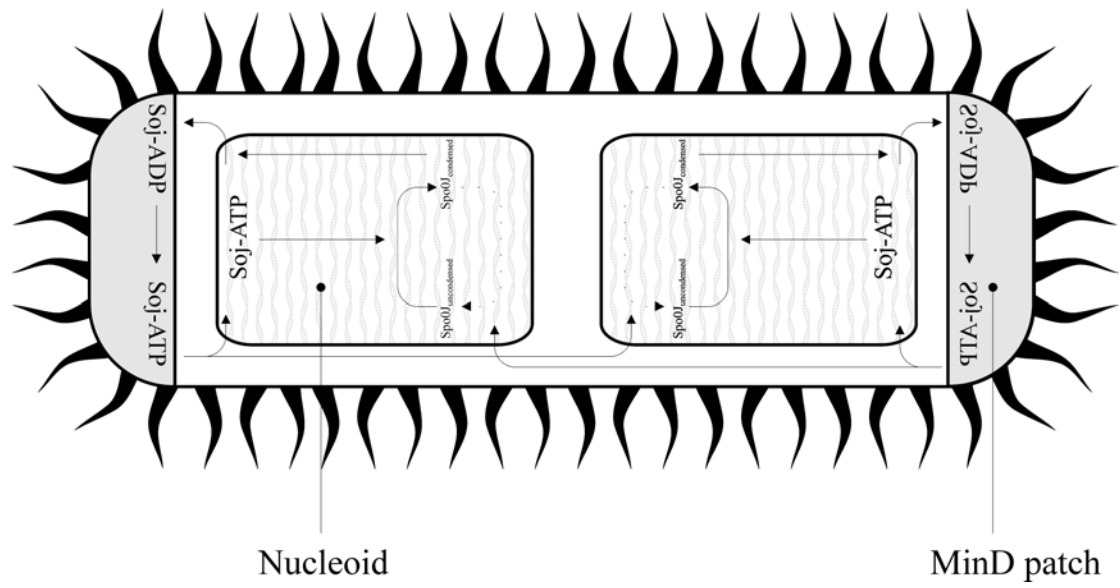Zhabotinsky A. M. *Proc. Acad. Sci*., USSR, 157, 392. (1964)

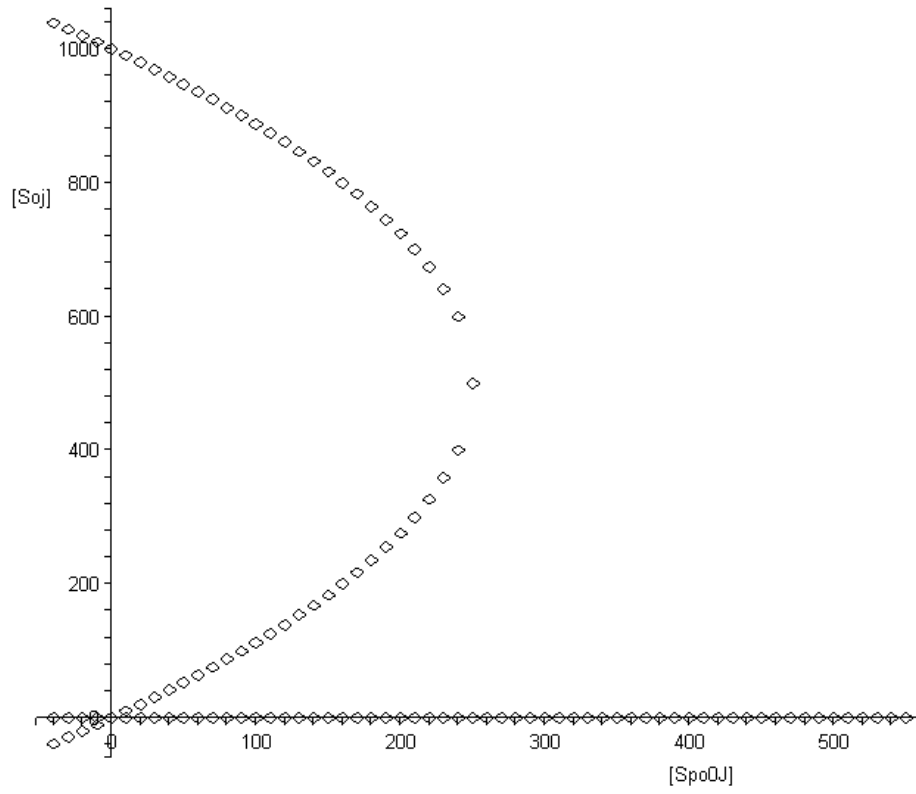Fig. 1. The mechanism of oscillations, rationalizing experimental facts.

Fig.2. Bifurcation diagram for our system. Circles specify steady state concentrations of bound Soj for every given concentration of condensed Spo0J.
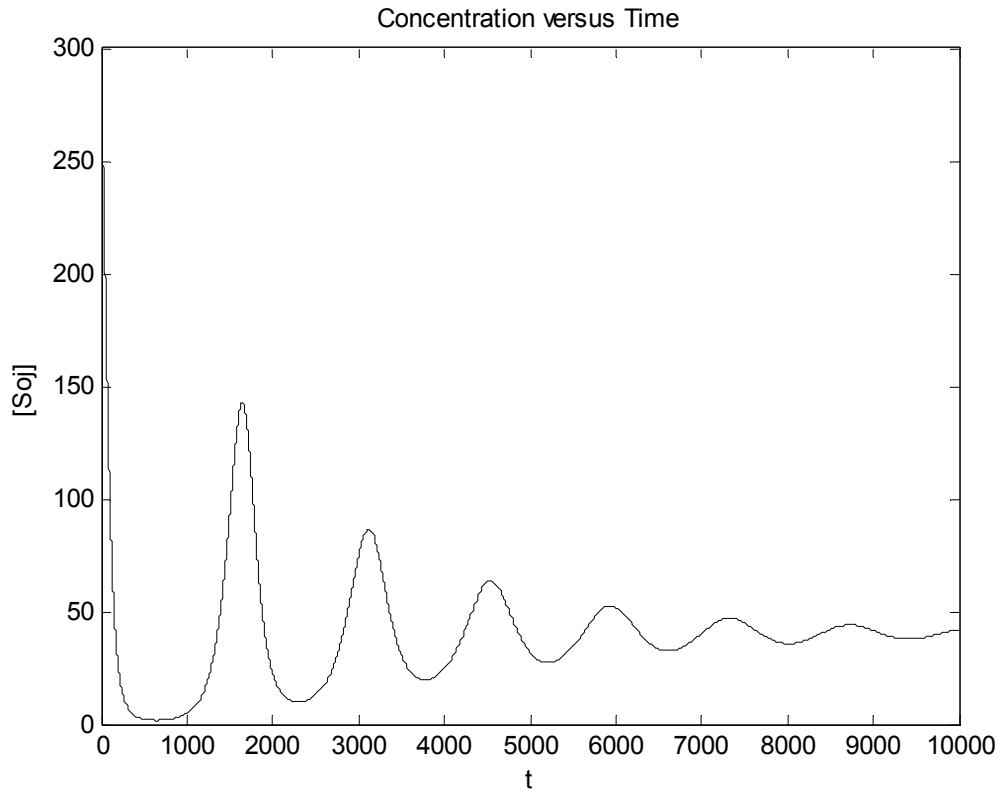
Fig. 3. Concentration versus time plot for the initial model, displaying transitory oscillations.
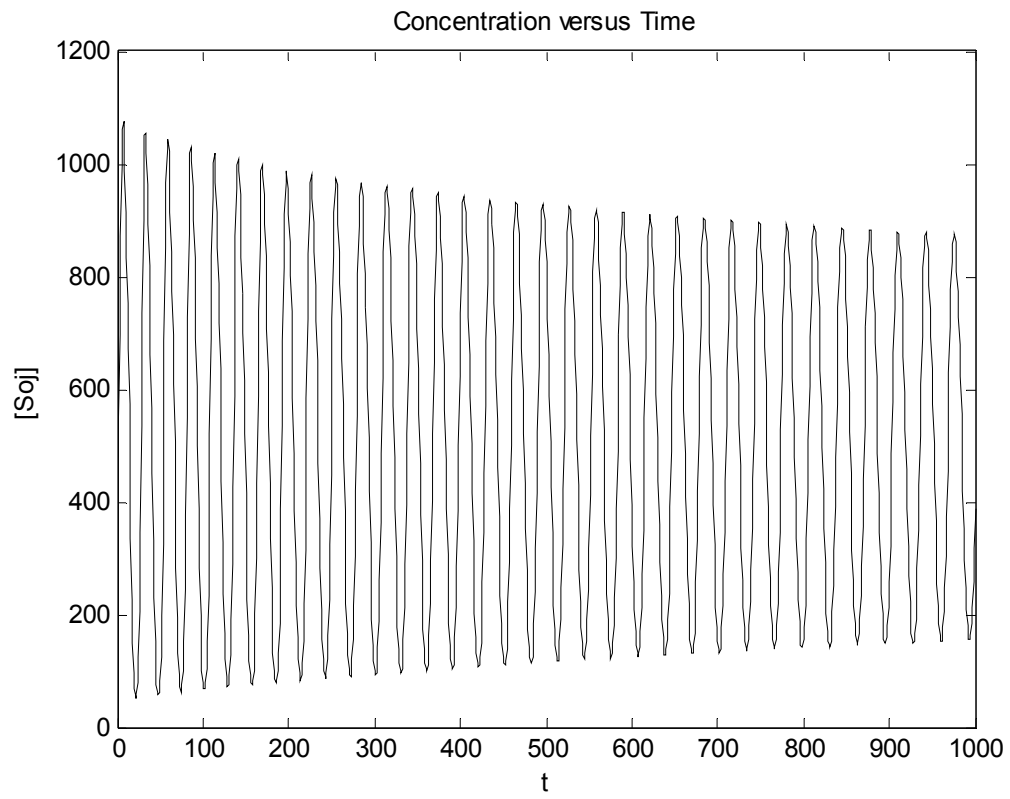
Fig 4. Modified model: transitory behaviour in the case of two coupled oscillators.
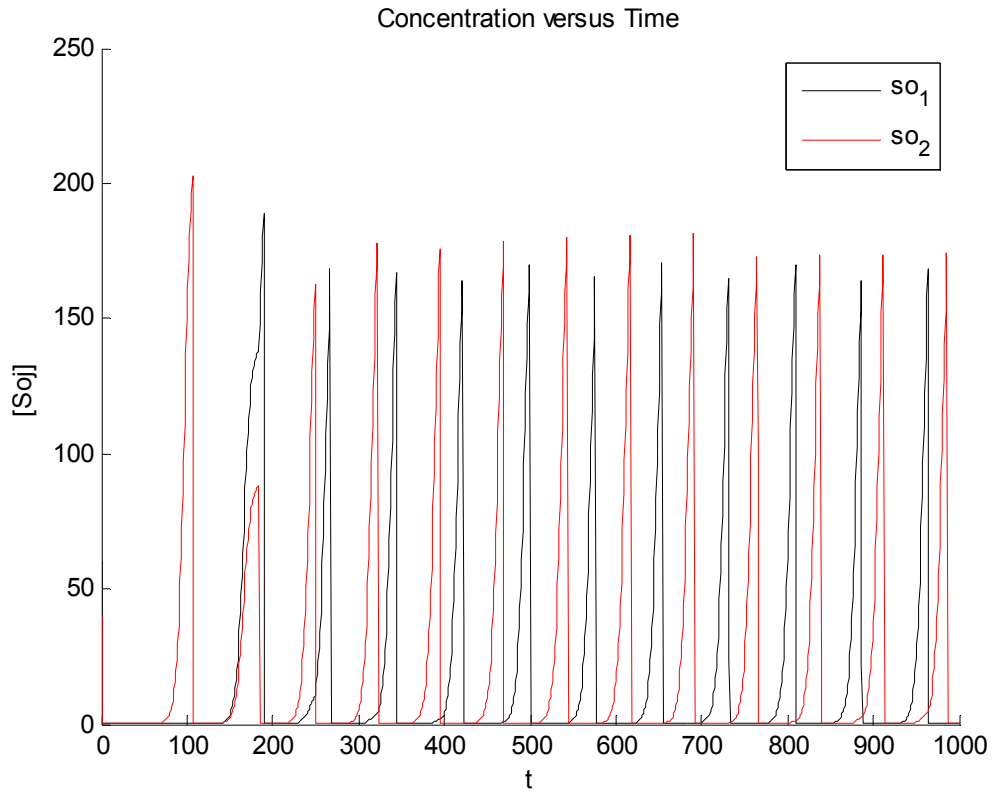
Fig. 5. Stable, irregular oscillations in the case of "unphysical" hysteresis.
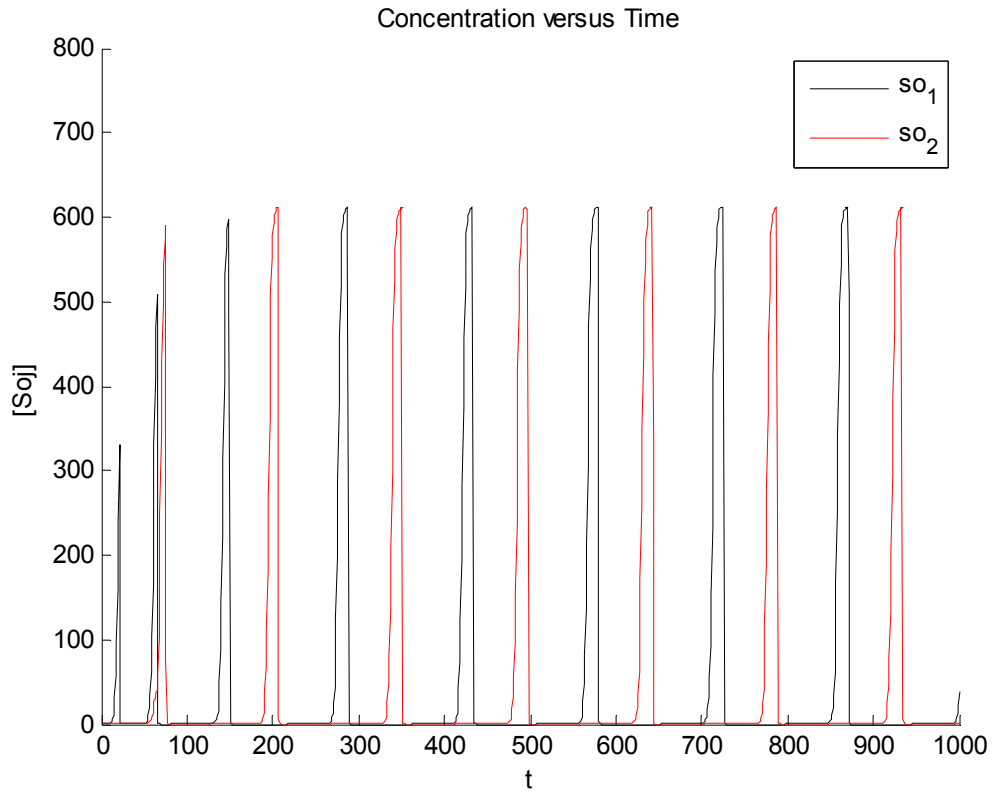
Fig. 6. Stable oscillations resulting from cooperativity in the Spo0J condensation-decondensation dynamics.
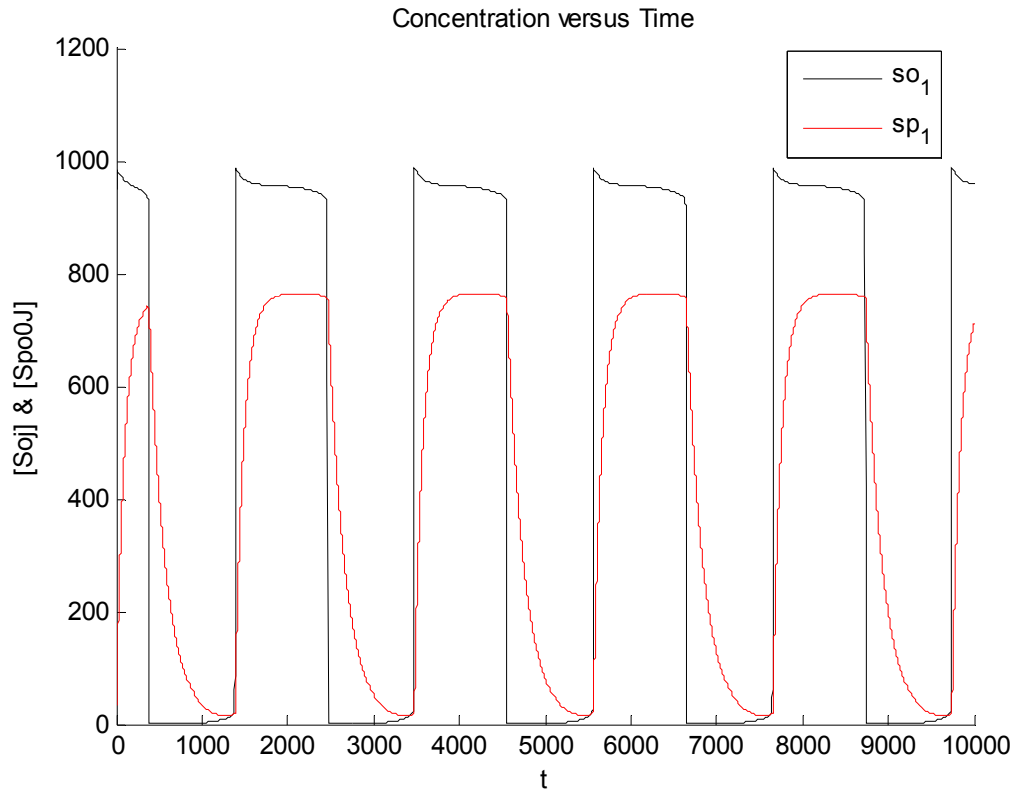
Fig. 7. Oscillations, resulting from cooperativity in Soj binding. so_1 denotes the concentration of Soj on the first nucleoid while sp_1 is the concentration of Spo0J. The peaks overlap, implying that these proteins are likely to colocalize in the PDE version of the same model, as was suggested by the experimental data.
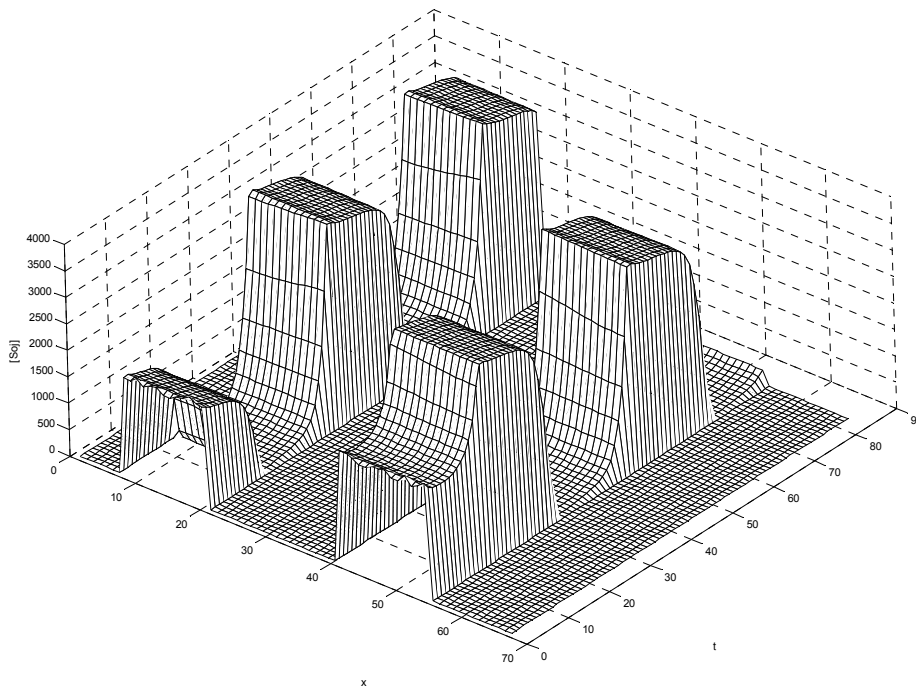
(a)
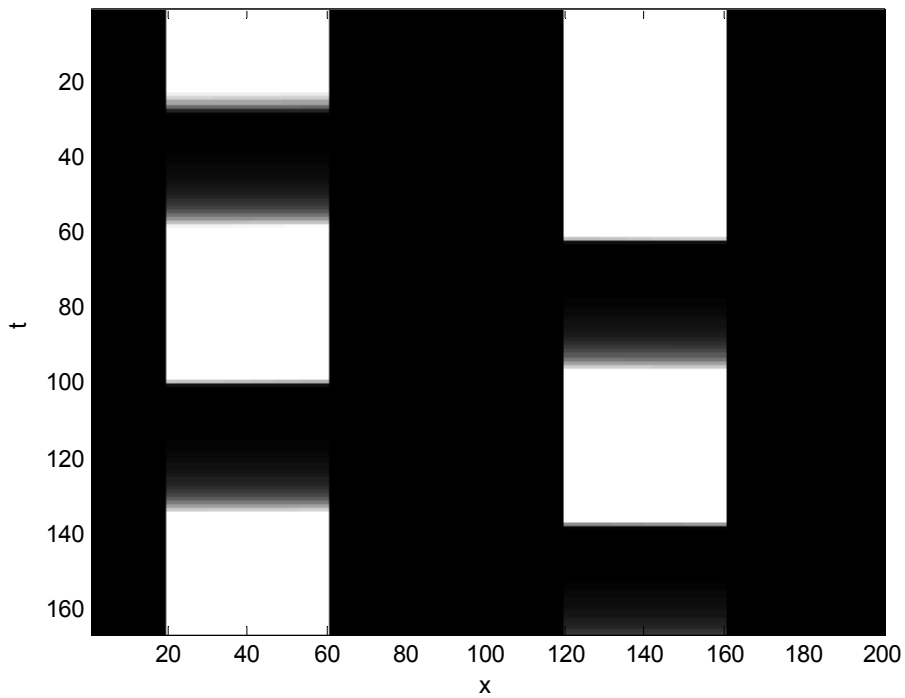
(b)

Fig. 8. Results of the PDE simulation. (a) Surface plot (b) The same plot viewed from above. White regions correspond to high concentration of bound Soj. Oscillatory behaviour is obvious.
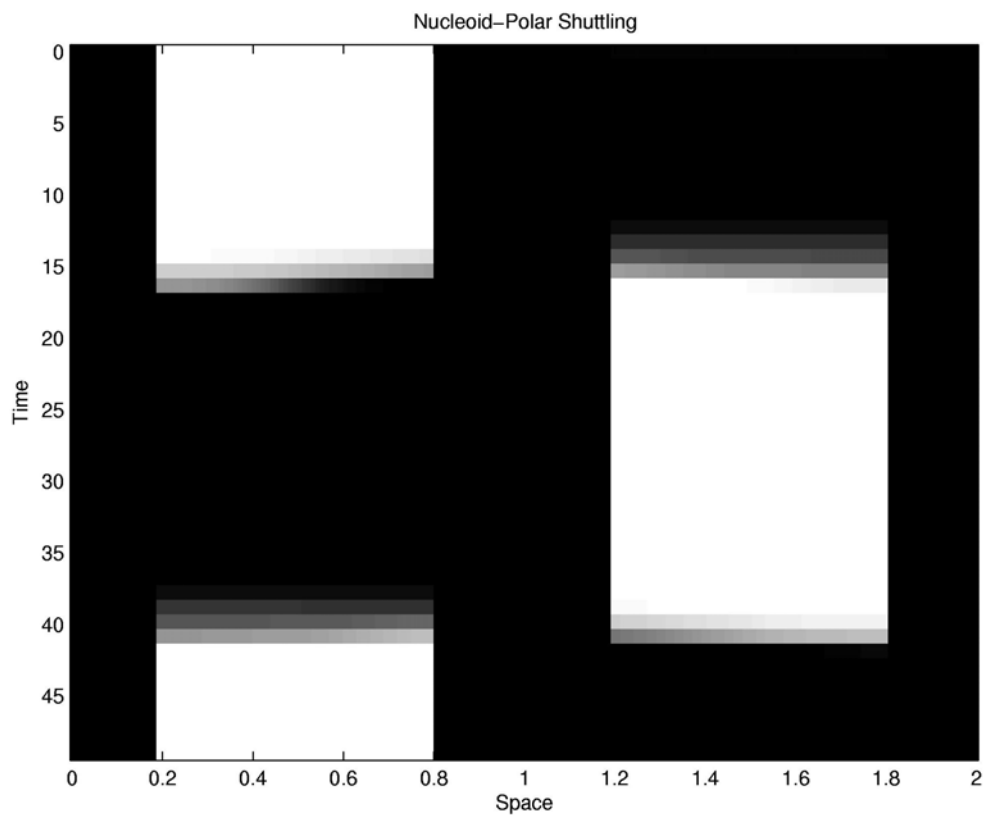
Fig. 9. Accounting for nucleoid-polar shuttling.
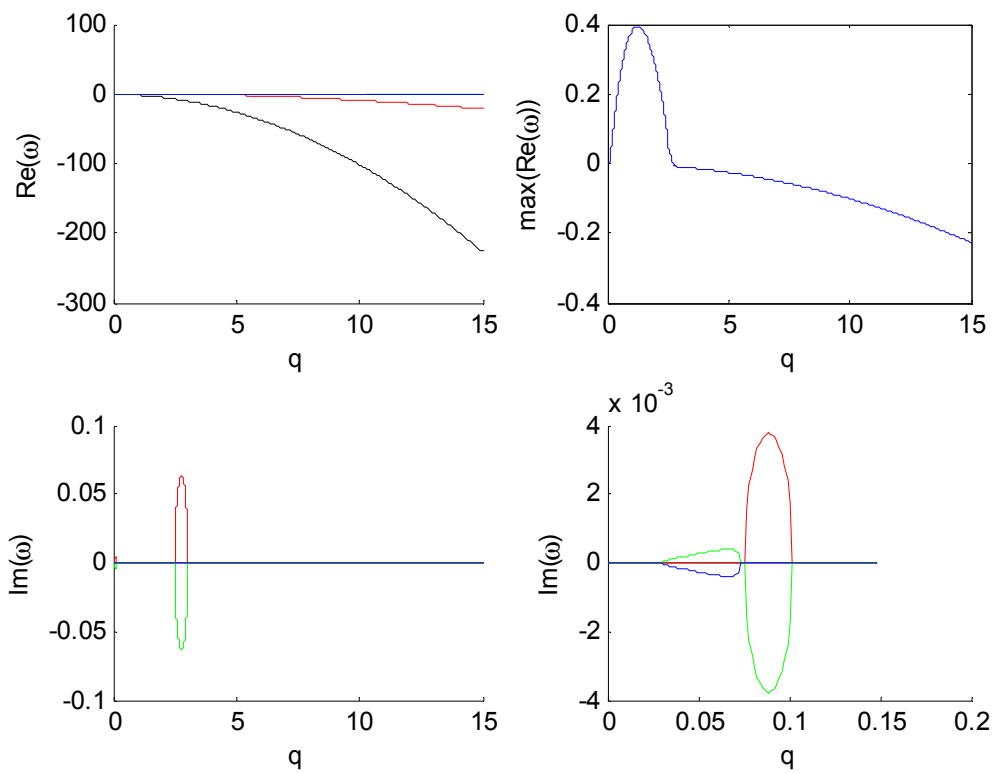
Fig. 10.   Eigenvalue spectrum and dispersion relationship for the PDE.
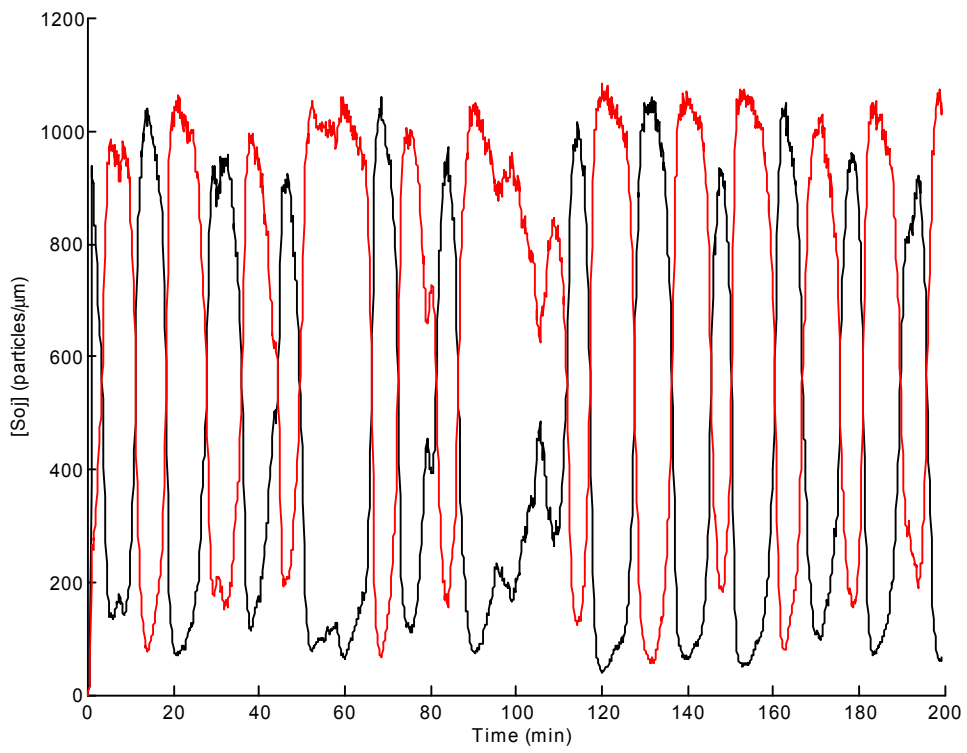
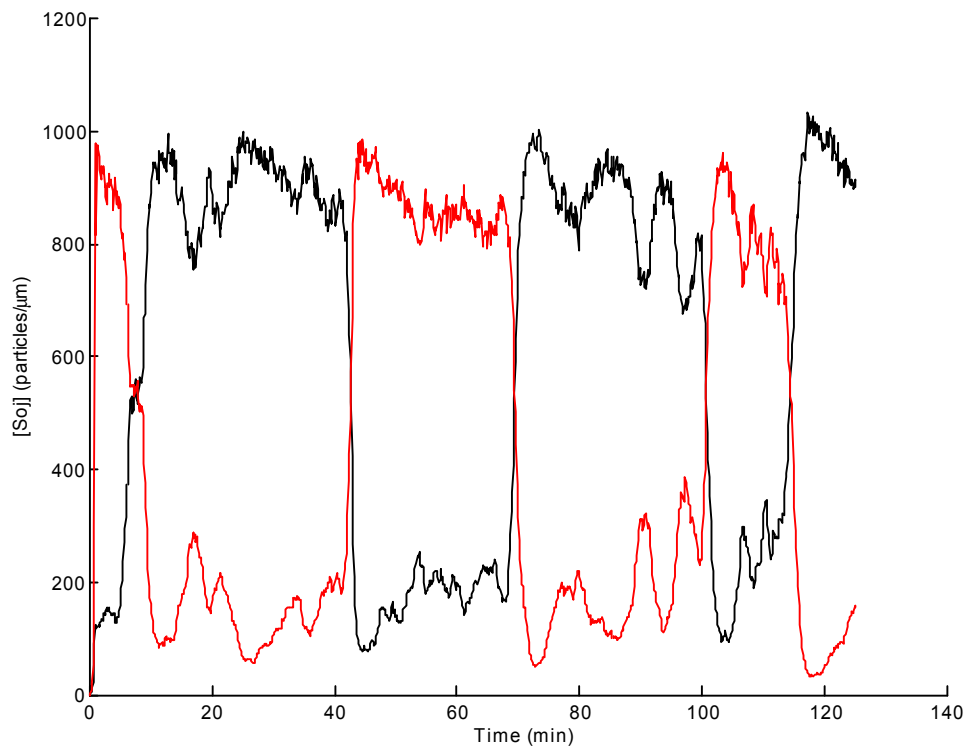Fig. 11.   Oscillations in the case of Spo0J mutant.

Fig 12.   Oscillations in the wild type cells. The period is approximately three
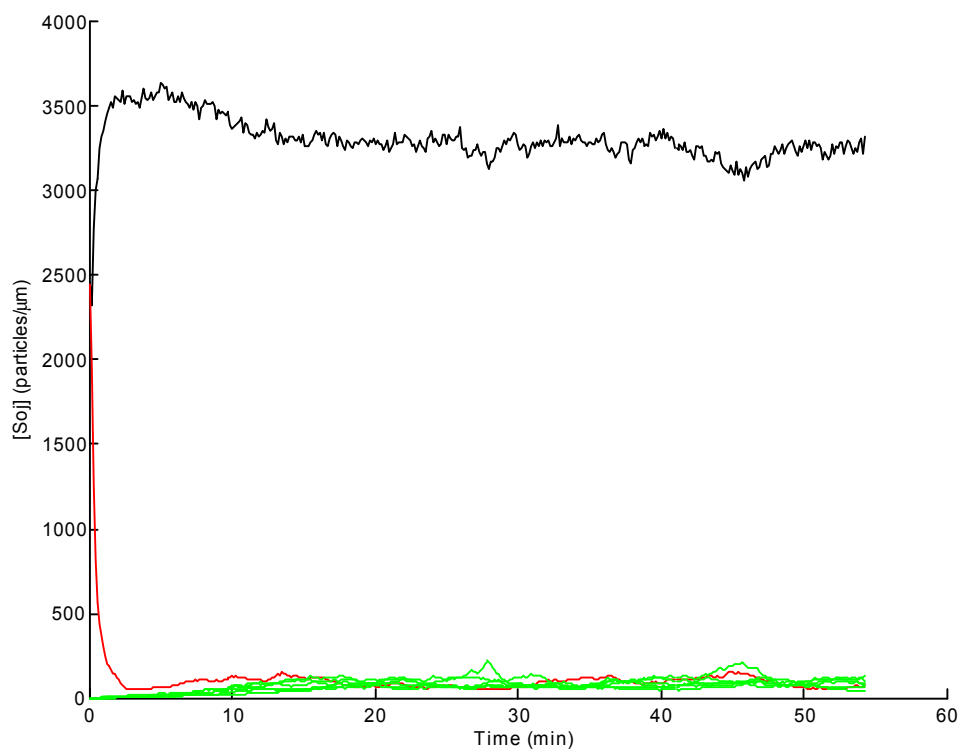   times grater then in the Spo0J mutant.

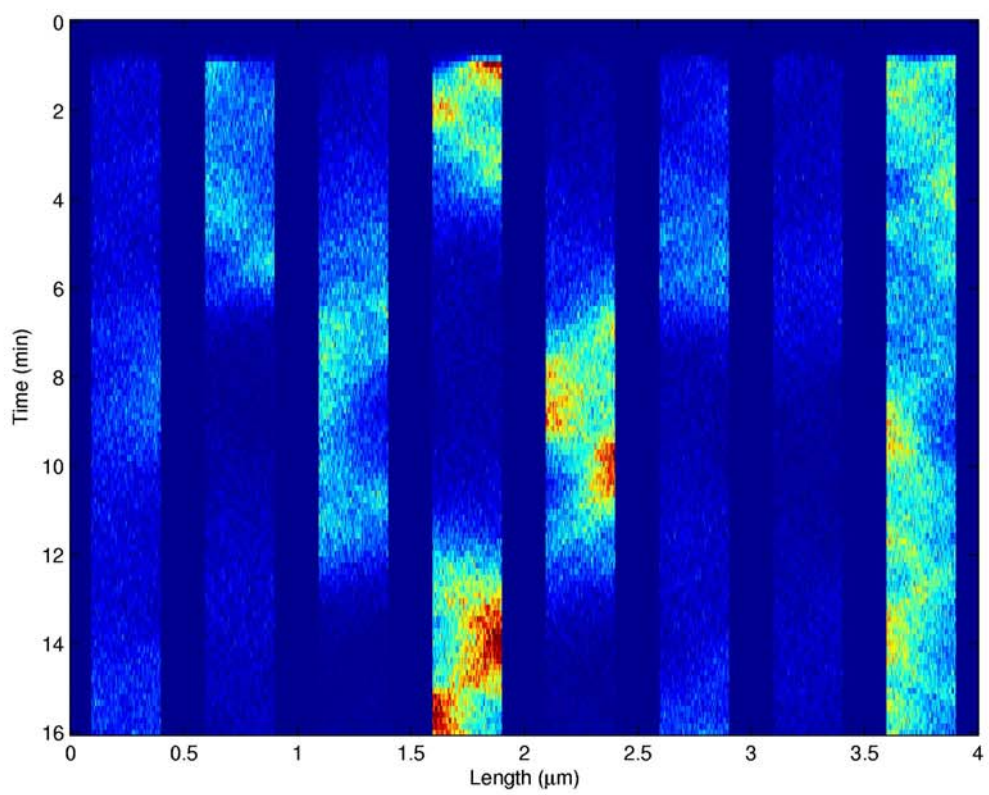Fig. 13.   No dynamics in the filamentous wild type cell, lacking FtsZ.

Fig. 14. Space-time plot of the concentrations in the filamentous Spo0J mutant. Distinct erratic relocations are observed.